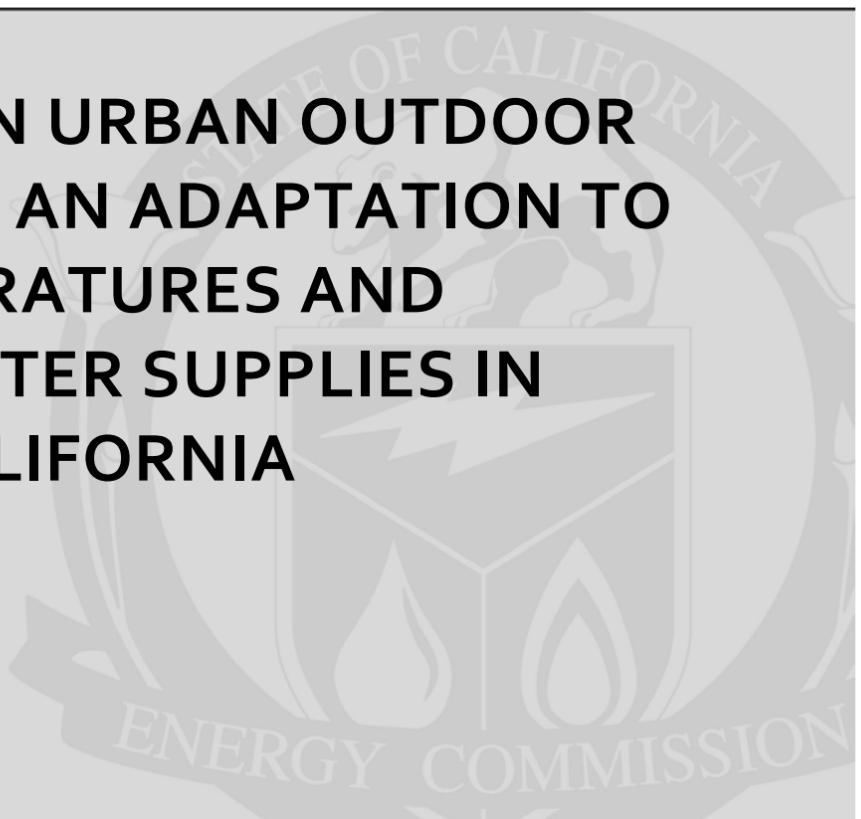


**Energy Research and Development Division
FINAL PROJECT REPORT**

**REDUCTIONS IN URBAN OUTDOOR
WATER USE AS AN ADAPTATION TO
RISING TEMPERATURES AND
DECLINING WATER SUPPLIES IN
SOUTHERN CALIFORNIA**



Prepared for: California Energy Commission
Prepared by: University of California

MARCH 2012

CEC-500-2013-152

PREPARED BY:

Primary Author(s):

Diane E. Pataki
Terri S Hogue
Stephanie Pincetl

University of California, Irvine
University of California, Los Angeles

Contract Number: PIR-08-005

Prepared for:

California Energy Commission

Joseph O'Hagan
Contract Manager

Linda Spiegel
Office Manager
Energy Generation Research Office

Laurie ten Hope
Deputy Director
ENERGY RESEARCH & DEVELOPMENT DIVISION

Robert Oglesby
Executive Director

DISCLAIMER

This report was prepared as the result of work sponsored by the California Energy Commission. It does not necessarily represent the views of the Energy Commission, its employees or the State of California. The Energy Commission, the State of California, its employees, contractors and subcontractors make no warrant, express or implied, and assume no legal liability for the information in this report; nor does any party represent that the uses of this information will not infringe upon privately owned rights. This report has not been approved or disapproved by the California Energy Commission nor has the California Energy Commission passed upon the accuracy or adequacy of the information in this report.

ACKNOWLEDGEMENTS

The authors thank N. Bijoor, C. Goedhart, L. Litvak, J. Kim, H. McCarthy, and D. Moering for contributions to data collection and analysis, and the Los Angeles Dept. of Water and Power for providing water consumption data.

PREFACE

The California Energy Commission Energy Research and Development Division supports public interest energy research and development that will help improve the quality of life in California by bringing environmentally safe, affordable, and reliable energy services and products to the marketplace.

The Energy Research and Development Division conducts public interest research, development, and demonstration (RD&D) projects to benefit California.

The Energy Research and Development Division strives to conduct the most promising public interest energy research by partnering with RD&D entities, including individuals, businesses, utilities, and public or private research institutions.

Energy Research and Development Division funding efforts are focused on the following RD&D program areas:

- Buildings End-Use Energy Efficiency
- Energy Innovations Small Grants
- Energy-Related Environmental Research
- Energy Systems Integration
- Environmentally Preferred Advanced Generation
- Industrial/ Agricultural/ Water End-Use Energy Efficiency
- Renewable Energy Technologies
- Transportation

Reductions in urban outdoor water use as an adaptation to rising temperatures and declining water supplies in southern California is the final report for the PIER project PIR-08-005 conducted by the University of California. The information from this project contributes to Energy Research and Development Division's Energy-Related Environmental Research Program.

For more information about the Energy Research and Development Division, please visit the Energy Commission's website at www.energy.ca.gov/research/ or contact the Energy Commission at 916-327-1551.

ABSTRACT

There is increasing evidence that climate change will exacerbate urban water shortages in southern California. A large proportion of household water use is applied outdoors for irrigation, so a potential response to decreasing water supplies is to promote changes in outdoor landscaping and irrigation regimes to reduce outdoor water use. Many urban landscapes are over-irrigated and there is a paucity of data on the average transpiration rates and water requirements of urban plants. This project involved making direct measurements of the transpiration rates of urban lawns, shrubs, and trees in the Los Angeles metropolitan area and evaluating the main factors determining spatial and temporal variability in plant water use. Results showed the transpiration rates of well-watered urban plants may vary by at least an order of magnitude depending on species and local conditions. Modeling was conducted on the transpiration and evapotranspiration at the plant, plot, neighborhood, and municipal scales using a variety of methods and computational models. The potential for water conservation was assessed through changes in outdoor landscaping such as changes in species composition, shading of lawns, decreases in irrigated vegetation density, and changes in irrigation technology. The results suggested that the methods most likely to contribute to significant outdoor water consumption reductions in southern California urban areas were: 1) removal of lawns or shading of lawns by large trees; 2) changes in irrigation technology, particularly soil moisture measurement-based irrigation systems; and 3) selection of low water use tree species, such as species adapted to non-riparian semi-arid or Mediterranean climates. A remote sensing-based modeling approach that can capture some of the high degree of spatial variability in water and energy balance that is characteristic of urban areas for large-scale analysis of evapotranspiration over the irrigated metropolitan area is also included in this report.

Keywords: evapotranspiration, hydrology, irrigation, Los Angeles, outdoor water use, sap flux, transpiration, urban water consumption, water conservation

Please use the following citation for this report:

Pataki, D.E., Hogue, T., Pincetl, S. (University of California) 2012. *Reductions in urban outdoor water use as an adaptation to rising temperatures and declining water supplies in southern California*. California Energy Commission. Publication number: CEC-500-2013-152.

TABLE OF CONTENTS

Acknowledgements.....	i
PREFACE.....	ii
ABSTRACT	iii
TABLE OF CONTENTS.....	iv
LIST OF FIGURES.....	v
LIST OF TABLES.....	vi
EXECUTIVE SUMMARY	1
Introduction	1
Project Purpose.....	1
Project Results.....	1
Project Benefits.....	3
CHAPTER 1: Introduction.....	5
1.1 Landscape irrigation as an adaptation to climate change.....	5
1.2 Uncertainties in assessing plant and landscape water use	6
CHAPTER 2: Measured Plant Transpiration in Los Angeles Urban Landscapes.....	8
2.1 Plant-level transpiration.....	8
2.1.1 Species differences in transpiration rates and water use efficiency.....	8
2.1.2 Database of plant transpiration.....	15
2.2 Plot-level transpiration.....	17
2.2.1 Urban forest transpiration	18
2.2.2 Transpiration of lawns and mixed vegetation cover	20
2.2.3 Lawn water budgets.....	24
CHAPTER 3: Remote Sensing and Ground-based Evapotranspiration Models for Los Angeles.....	29
3.1 Remote Sensing Model	29
3.1.1 UCLA-ET Algorithm	29
3.1.2 Remote Sensing Data.....	31
3.1.3 ET estimates for Los Angeles	32
3.1.4 Landscaping scenarios	36

3.2 ET measurements in the model domain	40
3.2.1 Study Areas.....	40
3.2.2 Measurements.....	42
3.2.3 Results and Discussion.....	47
3.3 Model-data comparisons.....	50
CHAPTER 4: Conclusions and Recommendations	53
4.1 Options for reducing outdoor water consumption.....	53
4.1.1 Species composition	54
4.1.2 Spatial configuration of landscape types.....	55
4.1.3 Climatic variability	55
4.1.4 Irrigation technology	55
4.2 Regional scale models	55
REFERENCES	57

LIST OF FIGURES

Figure 2.1: Measured whole tree water use in August by species and region of origin.....	10
Figure 2.2: Transpiration per unit leaf area of evergreen shrub species native to arid, temperate, or tropical habitats. All species were growing under common garden conditions at the.....	13
Los Angeles County Arboretum and Botanical Garden.....	13
Figure 2.3: Native ranges of horticultural tree species measured for	14
Water Use Efficiency in Los Angeles.....	14
Figure 2.4: Basal Area Increment (BAI) vs. transpiration of Los Angeles tree species	15
Figure 2.5: Water Use Efficiency (WUE) versus growing season precipitation	15
and Vapor Pressure Deficit in species native environment	15
Figure 2.6: Plot-level urban forest canopy transpiration (E_c) by species and site	19
Figure 2.7: Plot-level urban forest canopy transpiration (EC) modeled	20
as a function of tree density and species	20
Figure 2.8: ET measured gravimetrically with weighing lysimeters vs. chambers.....	22
Figure 2.9: ET measured with chambers (ET_{ch}) vs. modeled ET (ET_m) from CIMIS.....	23
Figure 2.10: ET of 100% turfgrass plots (black bars) and mixed tree-lawn plots (grey and white bars).....	24
Figure 2.11: Leaf stomatal conductance measured in the three lawns	26
Figure 2.12: Evapotranspiration of the three lawn types estimated with the chamber method (upper panel) and Penman-Monteith modeling based on direct measurements of stomatal conductance and LAI (lower panel) compared to reference ET calculated by CIMIS	27
Figure 2.13: Complete water budgets for the three experimental lawns using both chamber-based and Penman-Monteith based estimates of ET.	28

Figure 3.1: Flow chart of the UCLA-ET SEBAL-based model and implementation.	32
Figure 3.2: Land cover imagery from (a) QuickBird satellite (b) NOAA's Coastal Change Analysis Program (C-CAP) over the west area near Downtown Los Angeles. The spatial distributions for monthly ET average (mm/day) and relative frequency distributions (bin size: 0.3mm/day) from (c) the Landscape Model and (d) the MS-SEB Model for selected months. Also minimum (min), maximum (max), mean and standard deviation (std) are also given.	33
Figure 3.3: Timeseries of monthly precipitation (mm/month) (top) and monthly CIMIS reference ET (CIMIS ET _o - mm/month) (bottom) from the Glendale site. The monthly MS-SEB derived ET (mm/month) by land use/land cover types (i.e., Developed Area, Grass, Forest, Shrubland and Wetland) in the entire Los Angeles county.	35
Figure 3.4: (Left) Monthly ET (mm/month) by development intensity (i.e., High, Medium and Low intensity and Open space) and (Right) Annual ET (mm/year) by different developed intensity in entire Los Angeles county.	36
Figure 3.5: Los Angeles study domain with the UCLA SEBAL-based ET for study days 2/11 (winter), 6/14 (late spring) and 9/7(summer) in 2009.	37
Figure 3.6: Los Angeles study domain with select areas (Santa Monica, Hancock Park and the San Fernando Valley) used in sensitivity analysis of vegetation cover.	38
Figure 3.7: Example of spatial patterns resulting from vegetation sensitivity analysis in the San Fernando Valley domain.	39
Figure 3.8: Transect layouts and plan view of the sampled sites. A) Jesse Owens Mini Park in Reseda, CA. B) Whitnall Highway in North Hollywood, CA.	41
Figure 3.9: Example of using Gaussian function to complete the curve from Jesse Owens Mini Park on May 5, 2011. A) A plot of the calculated hourly ET from measured data. B) Resultant ensemble curves using a respective hourly ET point to solve the Gaussian equation. The areas under the curves are listed in millimeters in the legend. C) The finalized ET curve after choosing the most appropriate point and curve from the ensembles.	45
Figure 3.10: Scatter plots of MS-SEB ET against Chamber Measured ET at instantaneous satellite overpassed time (a and d), at daily average (b and e) and Scatter plot of MS-SEB ET against Chamber Regressed ET at daily basis (c and f) for Jesse Owens and Whitnall Highway, respectively. Also Bias, RMSE (Root Mean Square Error), and Pearson Correlation Coefficient (R) are also presented.	52

LIST OF TABLES

Table 2.1: Sap flux measurement sites and species	11
Table 2.2: Shrub species, family, and continent of origin of evergreen shrubs measured at the Los Angeles County Arboretum and Botanical Garden.	12
Table 2.3: Coefficients of the model described in equation (2.5).	17
Table 3.1: MODIS and Landsat satellite products and their spatial and temporal resolution used in the SEBAL-based UCLA-ET algorithm.	31
Table 3.2: Results from sensitivity analysis for three select locations. Table includes NDVI and ET results for a select study day in June, 2009.	40

Table 3.3: Past and present meteorological data from National Climatic Data Center gauges. The sampled period (Nov 2010-Oct 2011) is compared with the previous five water years. Thirty-year averaged historical data (1980-2010) is from the Western Regional Climate Center.....	41
Table 3.4: ET measurements recorded at the two parks From November 2010 to October 2011. Typically, three measurements were taken each month with a few exceptions. Measurements for Whitnall Highway began in January 2011. All values are in mm/day.....	47
Table 3.5: Seasonal Averages of ET for both parks.	48
Table 3.6: Published urban ET values from Grimmond and Oke (1999) compared to values in the current study. Published values are scaled to 90% vegetation cover for comparison to Jesse Owens and Whitnall Highway ET values.	49
Table 3.7: Jesse Owens seasonal model and reference ET rates used by LADWP (Repp, 2012) in millimeters. Modeled ET values span from Nov 2010-Oct 2011. Reference ET is from Jan 2010-Dec 2010.....	50

EXECUTIVE SUMMARY

Introduction

One of the most significant potential impacts of climate change on California is a reduction in the state's water supply. Modeled losses in snowpack in the Sierra Nevada due to climate warming are as high as 90 percent by the end of the 21st century, with decreases in water deliveries from the Delta as high as 50 percent. These changes will exacerbate the increasing pressures on water supplies from a growing population and from reductions in water extraction and delivery due to environmental concerns about habitat loss and endangered species. Declines in water supplies and increases in the frequency of drought are expected even under low greenhouse gas emission and climate warming scenarios. Adaptation strategies to cope with declining water availability through reductions in water demand are greatly needed. A large fraction of California's water consumption is used outdoors, so reductions in irrigation have a large potential for water conservation. While there has been emphasis on the potential for reducing irrigations rates in the agricultural sector, less attention has been paid to the potential for reducing urban outdoor irrigation.

Project Purpose

This project focused on evaluating the potential for reducing urban water demand in southern California through changes in outdoor water use. Very little direct information has been available about rates of evapotranspiration (ET) and the complete water budget of urban landscapes. While there is an assumed potential for water savings through improved irrigation efficiencies and changes in the species mix of urban plantings, the extent of possible water savings has not been thoroughly evaluated. The authors assessed current landscape water use and the potential for reducing end-user demand for water through changes in urban landscaping through direct measurements of transpiration in the Los Angeles area coupled with a remote-sensing based model. The researchers also sought to evaluate the effectiveness of encouraging low-water landscapes as an adaptation to climate change at both plot and municipal scales. This project provided some of the first direct measurements of urban plant and landscape water use in Los Angeles. The research team evaluated the efficacy of many possible methods of reducing outdoor water use through a series of observational, experimental, and modeling studies.

Project Results

There are few data available in the literature about the water use (transpiration) of urban plants *in situ*, although many effective methods are available for measuring plant transpiration. Urban landscapes contain unique assemblages of species and environmental conditions, so direct measurements of transpiration were needed to quantify landscape water use by location, particularly in irrigated areas. The authors used a variety of methods including sap flux measurements, porometry, and static chambers to measure the water use of different species and landscape types throughout the Los Angeles area. Porometry measures the degree of stomatal opening by means of resistance to the diffusion of water vapour. The researchers found that under the same well-watered conditions, the water use of mature urban trees in Los Angeles varied by an order of magnitude based on species differences in physiology. The authors also measured the Water Use Efficiency (WUE) of Los Angeles trees with a combination

of water use and stem growth measurements and found that slow growth rates and small tree size are not necessarily a consequence of low water use, as some species have both a large canopy size and high WUE. Notably, native riparian species such as the popular California sycamore have low WUE and very high water use. Selecting appropriate species for Los Angeles with high WUE (many of which are non-native) offers a means of including large shade trees in urban landscapes at a relatively low water cost.

The authors also measured transpiration of a variety of turfgrass species and found smaller differences among species. Evapotranspiration of turfgrass was not very sensitive to the choice of turfgrass type and ET rates of irrigated turfgrass in full sun were very high relative to other landscape types. However the presence of shade trees significantly decreased total landscape ET containing turfgrass. Shading appeared to have a significant effect on lawn water use that is larger than the amount of water consumed by the added trees. In addition, the researchers tested three lawn irrigation technologies including a conventional system with an automated timer, an irrigation system triggered by readings from soil moisture sensors, and a weather station-based system tied to the California Irrigation Management Information System (CIMIS). The soil moisture sensor-based system was the most efficient system, resulting in the lowest water consumption and the smallest water losses from drainage and surface runoff. A combination of shading of lawns and new irrigation technologies showed great potential to reduce the water consumption of turfgrass landscapes.

The authors utilized an ET model based on satellite remote sensing inputs to capture the high degree of spatial variability in ET characteristic of urban landcover. They compared model outputs to ground-based ET measurements and found reasonable agreement under most conditions. The model was then used to evaluate the impacts of scenarios of vegetation change on total urban ET and municipal water consumption. This evaluation showed that turfgrass ET may constitute approximately one-sixth of the total water consumption of Los Angeles. There would be a larger proportional reduction in ET in the hot and dry inland areas than near the coast if urban leaf area were reduced by 50 percent. In these model scenarios ET was reduced by 34 percent in the San Fernando Valley and 13 percent in Santa Monica. A simple projection for the city of Los Angeles implied reduced municipal water consumption of approximately 10 percent with reduced irrigated leaf area of 50 percent. This analysis did not discriminate among vegetation types as that was not possible with the current datasets. Further work will differentiate among specific landscape and vegetation types to separately evaluate the impact of turfgrass, tree species, and other types of common urban landscaping on municipal water use.

Urban outdoor water use and ET are often modeled using simple methods that seldom account for the diversity of urban landscapes and the unique environmental conditions in irrigated cities. The research team's direct measurements of plant water use and ET in Los Angeles revealed some unexpected patterns that are contrary to common assumptions about the appropriate species to plant in southern California. The authors provided a database of transpiration rates of common species under varying environmental conditions and recommendations for species combinations and landscape types that would result in lower water consumption. Modeling frameworks that fully account for the complexity of urban landscapes are still being developed, but remote sensing-based approaches that can assimilate higher resolution and multispectral products as they become available have a great deal of promise for modeling ET in complex terrain. A combination of measurement and modeling approaches could provide detailed information about the options for coping with declining available water for outdoor urban use in California.

Project Benefits

This study provided a scientific basis for developing strategies for reducing urban water demand as an adaptation strategy in a changing climate. This research project was an important and necessary step in synthesizing crucial information on plant water-usage in urban landscapes so that government agencies and other interested parties in California can use this information for water conservation purposes.

California's water supplies may be severely impacted by future climate change. Because water is closely tied to energy production, implementing water conservation measures as an adaptation to climate change will help reduce the associated impacts on energy demand and generation. This research will help ensure that secure, stable, and reliable sources of energy can continue to be provided to California's residents.

CHAPTER 1:

Introduction

1.1 Landscape irrigation as an adaptation to climate change

One of the most significant potential impacts of climate change on California is a reduction in the state's water supply. Modeled losses in snowpack in the Sierra Nevada due to climate warming are as high as 90 percent by the end of the 21 century, with decreases in water deliveries from the Delta as high as 50 percent (Cayan et al. 2006). These changes will exacerbate the increasing pressures on water supplies from a growing population and from reductions in water extraction and delivery due to environmental concerns about habitat loss and endangered species. Even under low greenhouse gas emission and climate warming scenarios, declines in water supplies and increases in the frequency of drought are expected, such that adaptation strategies to cope with declining availability through reductions in water demand are greatly needed. As a large fraction of California's water consumption is used outdoors, reductions in irrigation have large potential for water conservation. While there has been emphasis on the potential for reducing irrigations rates in the agricultural sector, less attention has been paid to the potential for reducing urban outdoor irrigation. Yet, 35 percent to 65 percent of household water use in southern California is used outdoors (Gleick et al. 2003).

This project focused on evaluating the potential for reducing regional water demand through changes in outdoor water use. Very little direct information has been available about rates of evapotranspiration and the complete water budget of urban landscapes, particularly at municipal to regional scales. While there is assumed to be a potential for water savings through improved irrigation efficiencies and changes in the species mix of urban plantings, the extent of possible water savings has not been thoroughly evaluated. Much uncertainty remains about the water budget of urban landscapes and the proportion of irrigation water actually used in transpiration vs. other water losses (evaporation, drainage, runoff), even under current climate scenarios. In addition, plant water demand, evaporation rates, and soil moisture are likely to change as temperatures increase, further complicating predictions about the effectiveness of programs to reduce outdoor water use.

Through direct measurements of transpiration in the Los Angeles area coupled with a remote-sensing based model, we assessed current landscape water use and the potential for reducing end-user demand for water through changes in urban landscaping. We sought to evaluate the effectiveness of encouraging low-water landscapes as an adaptation to climate change at both plot and municipal scales. Ironically, a commonly proposed adaptation to climate change in cities is an increase in tree-planting programs to increase carbon sequestration, yet most urban trees in southern California require irrigation. Therefore, we assessed the tradeoff between C sequestration in urban trees and their water use. The project components included: developing a database of measured transpiration rates of urban landscaping plants *in situ*; scaling these data to the plot level in order to evaluate species and compare outdoor irrigation rates to plant water use; development and validation of a model of urban evapotranspiration across the Los Angeles region; utilization of the model to assess scenarios of large-scale changes in urban

landscaping and irrigation. We worked directly with the Los Angeles Dept. of Water and Power to obtain residential water consumption data, evaluate current water management practices, and disseminate the results of the study.

1.2 Uncertainties in assessing plant and landscape water use

There has been very little direct information available about the water use of urban plants. Recommendations for water-conserving landscapes are generally based on anecdotal information, or on the water use of a given species in its native, non-irrigated environment. This leaves a large information gap about rates of evapotranspiration (ET) in irrigated urban cities, despite the fact that ET is an important component of the local hydrological budget and climate system. There is also a virtually complete lack of information about the partitioning of ET between plant transpiration and soil/surface evaporation. Studies suggest that most outdoor vegetation is over-irrigated and water is often applied in excess of plant requirements (Kenney et al. 2004; Robbins and Birkenholtz 2003), such that a large fraction of applied water likely evaporates, flows directly into storm drains, or percolates below the rooting zone.

Given the lack of data on urban landscape water use and fluxes, and the relationship between urban vegetation and regional hydrology, it is very difficult to provide quantitative estimates of the potential for large-scale changes in outdoor landscaping and irrigation to respond effectively to declining water supplies. There are complex feedbacks between surface water fluxes and climate that have yet to be addressed in irrigated cities. ET is an important component of the surface energy budget that affects energy balance, sensible heat flux, and therefore air temperature. Changes in local air temperature as a result of changes in outdoor irrigation are a critical feedback to greenhouse gas emissions and climate change, as air temperature is strongly correlated with building energy use (Le Comte and Warren 1981; Lehman and Warren 1978; Quayle and Diaz 1980). It is very likely that urbanization in southern California has dramatically changed ET, as conversions to urban land cover in California are often associated with replacing semi-arid and arid vegetation with a variety of non-native trees, turfgrass, and other vegetation that require heavy irrigation. Typical ET rates of well-watered grasses and deciduous forests are $> 3\text{--}5 \text{ mm d}^{-1}$ (Meyers 2001; Pataki et al. 2005; Wilson and Baldocchi 2000), while those of semi-arid and arid ecosystems are an order of magnitude smaller. Average Bowen ratios (ratio of sensible to latent heat fluxes) of deciduous forests are approximately 0.4, while ecosystems in Mediterranean climates can have Bowen ratios as high as 5 or more during the dry season (Wilson et al. 2002). Hence, urbanization in semi-arid areas can be associated with increased vegetative cover and greatly reduced Bowen ratios, which will change the surface energy budget and likely influence air temperature, wind patterns, and other aspects of local meteorology in addition to regional hydrology.

Ngo and Pataki (2008) utilized datasets on water imports and allocation in Los Angeles County to construct a regional water balance for 1990 and 2000. They reported that 1600 million metric tons (MMT) of water was imported into Los Angeles County in 2000, while 775 MMT was extracted from groundwater for municipal use. 930 MMT of water was accounted for in wastewater discharge, which is only 40 percent of total water extractions and imports. It is likely that a large portion of the remaining water is accounted for in ET (as opposed to

groundwater recharge and runoff) due to high rates of irrigation and high potential ET in the urban portion of the county. This calculation highlights the potential for reductions in outdoor water use to conserve appreciable amounts of water and greatly lower end user water demand on a regional basis. However, insufficient data were available in that study to complete the regional water budget due to uncertainty about water fluxes from irrigated urban land cover. By combining direct measurements and state of the art models, we can complete the local water budget and also evaluate scenarios of future change – both with regard to effects of climate change on local temperature and evaporative demand, and also incorporating scenarios of large scale changes in urban outdoor water use and their effectiveness in reducing water demand in the MWD service area.

CHAPTER 2:

Measured Plant Transpiration in Los Angeles Urban Landscapes

We measured transpiration *in situ* in a variety of residential, street, park, and institutional landscapes in the Los Angeles metropolitan area. We used three primary methods: 1) constant heat sap flux gauges for monitoring transpiration rates of mature trees in real time; 2) portable gas exchange systems for measuring leaf-level transpiration in smaller woody vegetation such as shrubs; and 3) clear, static chambers for measuring the ET rates of urban lawns. For most of the species and locations we studied these are the first direct measurements of transpiration and ET in urban, irrigated settings. To compare and contrast these results and to incorporate these data into estimates and models of plot-level and regional ET, we assembled a database of species-specific responses of transpiration to climatic variables, particularly vapor pressure deficit (VPD) and overstory incident radiation (I_o), which drive transpiration. We then utilized these results to estimate plot-level transpiration for urban forests and mixed landscape types as a function of species composition, tree density, and tree cover. We also evaluated the Water Use Efficiency (WUE) of urban trees to assess the water costs of utilizing trees to sequester carbon for climate change mitigation.

2.1 Plant-level transpiration

2.1.1 Species differences in transpiration rates and water use efficiency

The water use of mature trees can be monitored in real time by measuring heat dissipation in the boles (tree trunks). The temperature difference between heated and unheated probes has been empirically related to the flux of water through stems and boles by Granier (1987). This “sap flux density” is equivalent to transpiration of the canopy when the storage of water in stems is negligible, which is generally true on a daily time scale (Phillips et al. 1997). Therefore, we measured sap flux density on a half hourly time scale and integrated these measurements to obtain estimates of daily transpiration for each measured tree. To characterize transpiration rates of a particular species at a particular site, we monitored sap flux density in 5-12 individuals of the same species per site (depending on the number of individuals available) and reported the average and standard error. The data were recorded by dataloggers (CR10X, CR1000, and CR3000, Campbell Scientific Inc., Logan, UT, USA) every 30 seconds, and average values stored every 30 minutes. Sap flux density in the outer 2 cm of sapwood (J_o , g cm⁻²s⁻¹) was calculated following Granier (1987):

$$J_o = 119 \left(\frac{\Delta T_{max} - \Delta T}{\Delta T} \right)^{1.231} \quad (2.1)$$

where ΔT is the temperature difference between the probes, and ΔT_{max} is the maximum measured temperature difference, which was estimated from nighttime values when there was

no sap flux. We assumed that the zero sap flux condition was met when the nighttime VPD was lower than 0.2 kPa. Whenever nighttime VPD was higher than 0.2 kPa, we used ΔT_{max} from the previous night for calculating J_o .

As J_o is reported per unit sapwood (the active, transpiring portion of the stem), we needed estimates of the total cross-sectional sapwood area to estimate whole tree transpiration. Therefore, following the sap flux measurement period we cored the trees and visually determined sapwood area. To account for radial trends in sap flux, i.e., reductions in sap flux with sapwood depth, we utilized the functions developed by Pataki *et al.* (2011):

$$J_i = 1.033 J_o \exp\left(-0.5\left(\frac{x - 0.09963}{0.4263}\right)^2\right) \text{ for angiosperms, and} \quad (2.2)$$

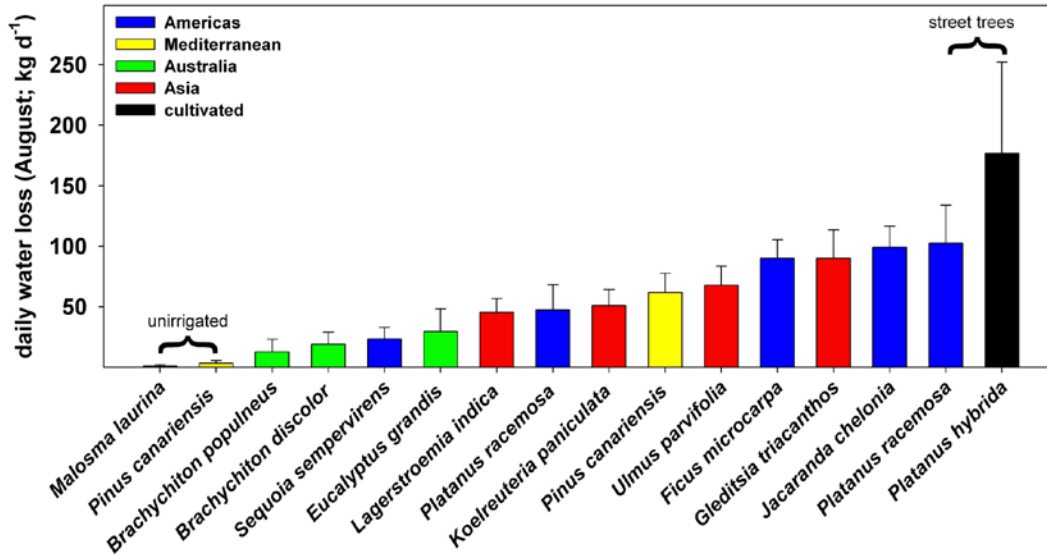
$$J_i = 1.257 J_o \exp\left(-0.5\left(\frac{x + 0.3724}{0.6620}\right)^2\right) \text{ for gymnosperms.} \quad (2.3)$$

where x is the normalized depth of each sapwood increment ($0 \leq x < 1$), J_o is the sapflux density of the outer 2 cm of sapwood (Eq. 1), and J_i is the resulting sapflux density in i -th increment. We summed sapflux densities in all depth increments to obtain whole tree transpiration (E_w , kg day⁻¹):

$$E_w = 10^{-3} \sum_{i=0}^n A_i J_i \quad (2.4)$$

where A_i is the cross sectional area of sapwood increments in cm².

Figure 2.1: Measured whole tree water use in August by species and region of origin



A list of measured species and locations is given in Table 2.1. In general, species differences in E_w were very large (Figure 2.1). Not surprisingly, unirrigated trees showed very low E_w ; however, more surprisingly, even well-irrigated trees showed enormous differences in E_w of about an order of magnitude. Since most trees in Los Angeles are non-native, we noted the region of origin of each species to determine if native species showed lower water use than non-native species. However, this was not the case. Species native to North America and to California in particular (eg. *Platanus racemosa*, the California sycamore) showed some of the highest rates of transpiration. In contrast, Australian species showed some of the lowest rates, including *Brachychiton* and *Eucalyptus*. The highest average E_w values were of the order of 100 kg water day⁻¹tree⁻¹, shown by the following groups of trees: *Ficus microcarpa* (102.7 ± 18.6), *Gleditsia triacanthos* (93.7 ± 26.2), *Platanus hybrida* (91.5 ± 37.0), *Jacaranda chelonina* (83.3 ± 24.0), and *Koelreuteria paniculata* (71.3 ± 33.8). The lowest E_w were of the order of 10 kg water day⁻¹tree⁻¹ and included *Quercus agrifolia* (8.7 ± 5.7), *J. mimosifolia* (10.9 ± 5.6), *Sequoia sempervirens* at the Los Angeles Police Academy (10.9 ± 5.8), *Eucalyptus grandis* at the University of California, Irvine (13.3 ± 10.6), *Brachychiton populneus* (13.8 ± 8.5), and *Pinus canariensis* at the Los Angeles Zoo (14.7 ± 4.5).

Table 2.1: Sap flux measurement sites and species

Site	Location	List of species	Comments
Audubon Starr Ranch Sanctuary (STR)	33°37' N 117°33' W	<i>Platanus racemosa</i> <i>Quercus agrifolia</i>	Non irrigated riparian forest; herbaceous understory
Fullerton Arboretum (FUL)	33°53' N 117°53' W	<i>Sequoia sempervirens</i>	Irrigated; no understory
Los Angeles Arboretum and Botanic Garden, Australian section (LAA)	34°08' N 118°03' W	<i>Brachychiton discolor</i> <i>Brachychiton populneus</i> <i>Eucalyptus grandis</i>	Irrigated; little or no understory; other isolated tree species present
Los Angeles Arboretum and Botanic Garden, South American section (LAS)	34°08' N 118°03' W	<i>Ficus microcarpa</i> <i>Gleditsia triacanthos</i> <i>Jacaranda chelonja</i> <i>Koelreuteria paniculata</i> <i>Lagerstroemia indica</i>	Irrigated; little or no understory; other isolated tree species present
Los Angeles Police Academy (PA)	34°04' N 118°14' W	<i>Pinus canariensis</i> <i>Sequoia sempervirens</i> <i>Ulmus parvifolia</i>	Irrigated; herbaceous understory
Los Angeles, residential street (SS)	34°04' N 118°20' W	<i>Platanus hybrida</i> <i>Platanus racemosa</i>	Not irrigated; trees in sidewalk insets
Los Angeles Zoo and Botanical Gardens (LAZ)	34°08' N 118°17' W	<i>Jacaranda mimosifolia</i> <i>Pinus canariensis</i>	Partially irrigated; herbaceous understory
University of California, Irvine (UCI)	33°38' N 117°50'	<i>Eucalyptus grandis</i> <i>Pinus canariensis</i> <i>Platanus racemosa</i> <i>Sequoia sempervirens</i>	Irrigated; groundcover of turfgrass, ivy (<i>Hedera helix</i>), ice plant (<i>Carpobrotus chilensis</i>), or herbaceous shrub

We also measured transpiration of some smaller woody vegetation. Because these measurements were not continuous they were not included in the transpiration database described below. However, these measurements were useful for evaluating assumptions about the water use of different types of species. Using a portable gas exchange system (LI-6400, Licor Inc, Lincoln, NE) we measured transpiration per unit leaf (E_L) of 21 evergreen shrub species located at the Los Angeles County Arboretum and Botanical Garden in Arcadia, CA. The plants were all grown in well-irrigated, horticultural settings in what may be considered a “common garden” – a setting in which species from different environments are grown in the same environmental conditions to assess genetic differences in plant characteristics such as water use. We measured transpiration on sun leaves of three individuals from each species. The selected

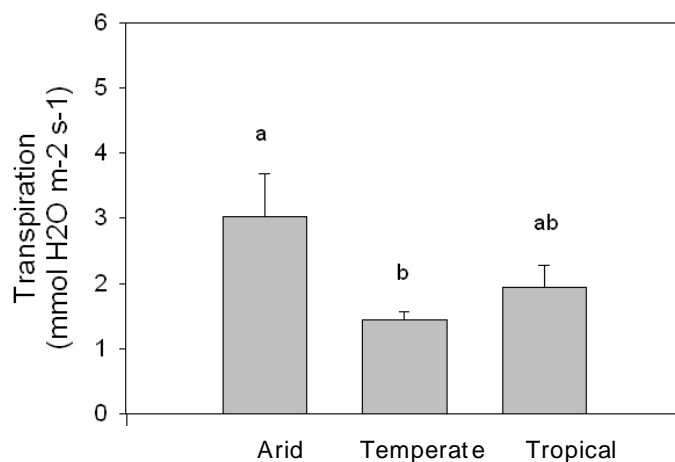
species varied in evolutionary history and region of origin, with species originating from arid, temperate, and tropical environments (Table 2.3).

Table 2.2: Shrub species, family, and continent of origin of evergreen shrubs measured at the Los Angeles County Arboretum and Botanical Garden.

Taxon	Family	Native Continent
Arid		
<i>Eremophila glabra</i>	Myoporaceae	Australia
<i>Grevillea rosmarinifolia</i>	Proteaceae	Australia
<i>Rosmarinus officinalis</i>	Lamiaceae	Europe
<i>Euryops pectinatus</i>	Asteraceae	Africa
<i>Euclea pseudebenus</i>	Ebenaceae	Africa
<i>Rhigozum obovatum</i>	Bignoniaceae	South America
<i>Senna artemisioides</i>	Fabaceae	Australia
Temperate		
<i>Dovyalis caffra</i>	Salicaceae	Africa
<i>Escallonia bifida</i>	Escalloniaceae	South America
<i>Acca sellowiana</i>	Myrtaceae	South America
<i>Itea yunnanensis</i>	Grossulariaceae	Asia
<i>Acacia cyclops</i>	Fabaceae	Australia
<i>Athanasia acerosa</i>	Asteraceae	Africa
<i>Sannantha virgata</i>	Myrtaceae	Australia
Tropical		
<i>Psidium guineense</i>	Myrtaceae	Central/South America
<i>Citrus aurantium</i>	Rutaceae	Asia
<i>Graptophyllum excelsum</i>	Acanthaceae	Australia
<i>Senna surattensis</i>	Fabaceae	Australia
<i>Ardisia quinquegona</i>	Myrsinaceae	Asia
<i>Bauhinia galpinii</i>	Fabaceae	Africa
<i>Thevetia peruviana</i>	Apocynaceae	South America

We hypothesized that species originating from arid environments would have the lowest transpiration rates, but this was not the case. On the contrary, arid species showed high transpiration rates similar to tropical species, while temperate species showed the lowest transpiration (Figure 2.2). This is presumably because all plants were well-watered; therefore, our measured transpiration rates represent maximum values rather than responses to water stress, which would likely show a very different pattern in arid vs. temperate and tropical species. From an ecological perspective, high transpiration rates in well-watered, arid species are consistent with adaptations to dry environments. Desert plants must have high rates of gas exchange after infrequent rain events in order to maintain sufficient carbon balance for growth. In other words, desert plants have a high capacity for transpiration and photosynthesis because they must rapidly fix carbon after rain events in their natural habitat; this is discussed further in Goedhart et al. (2012). The implications of these results for landscape water management are that utilizing traditional “xeriscape” species in landscape design may not necessarily result in lower landscape water use unless irrigated appropriately. Arid species that are well-watered may in fact use even more water than species in traditional landscape designs. Arid species can better tolerate water stress than mesic species (species from wet environment), so they are still a good choice for low water landscapes, but appropriate irrigation practices must be employed in order to conserve water.

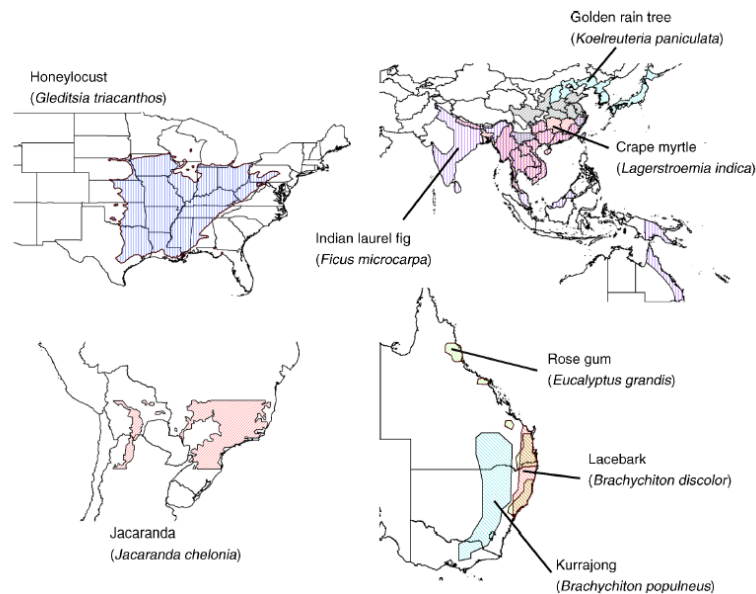
Figure 2.2: Transpiration per unit leaf area of evergreen shrub species native to arid, temperate, or tropical habitats. All species were growing under common garden conditions at the Los Angeles County Arboretum and Botanical Garden



Source: Goedhart et al. (2012)

Finally, we also assessed species differences in water use parameters by analyzing plant Water Use Efficiency (WUE), the carbon gained in growth per unit water lost in transpiration. This is a useful measure for several reasons: 1) species with low water use that are very slow growing are unlikely to popular landscape species, especially for trees; 2) carbon sequestration in trees has been cited as a potential climate change mitigation measure, but has potential water costs; and 3) WUE tends to be genetically controlled and may underlie species differences in transpiration. There are several methods for quantifying WUE including instantaneous, leaf-level measurements, carbon isotopes, and whole-tree measurements of water use and growth. A detailed discussion of the limitations and differences among these methods is found in McCarthy et al. (2011). Because the most direct and reliable method is to measure both whole tree water use and plant growth, we focus on those results here. Whole tree water use was measured in mature trees using the sap flux method described above. In several species we simultaneously measured the Basal Area Increment (BAI) of the bole using dendrometer bands, which record stem expansion.

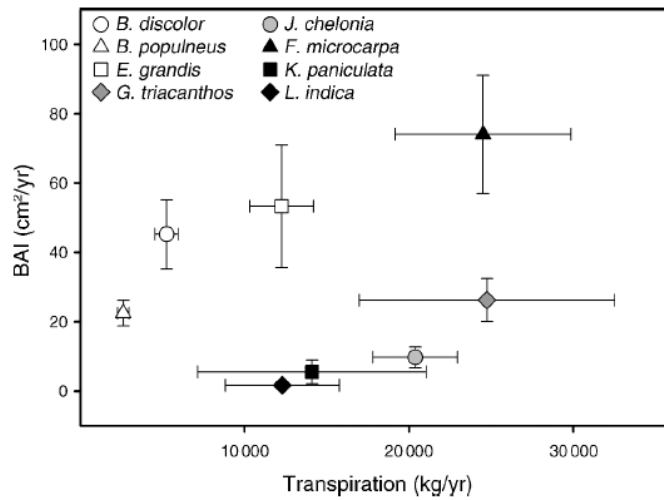
Figure 2.3: Native ranges of horticultural tree species measured for Water Use Efficiency in Los Angeles



Source: McCarthy et al. (2011)

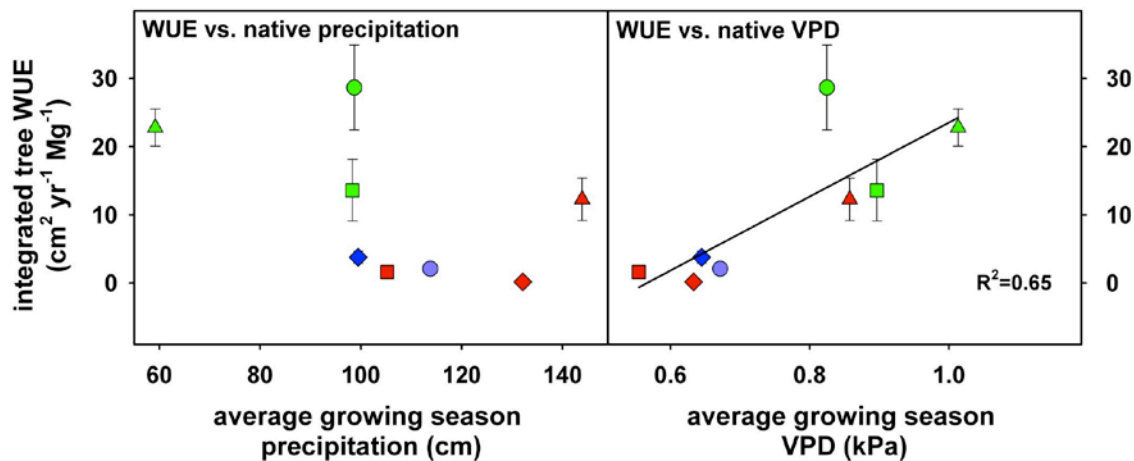
We determined the native ranges of species commonly grown in Los Angeles (Figure 2.3) and derived annual climate variables for the species' native environment, including growing season total precipitation and mean VPD. The studied species fell into two general categories of WUE, with *Brachychiton* spp., *Eucalyptus grandis*, and *Ficus microcarpa* (laurel fig) showing high BAI per unit water use (high WUE), and *Lagerstroemia indica* (crape myrtle), *Koelreuteria paniculata* (golden rain tree), *Jacaranda chelonina*, and *Gleditsia triacanthos* (honey locust) showing low BAI per unit water use (Figure 2.4). There was no relationship between WUE and the mean growing season precipitation of the species' native environment. However, differences in WUE were largely explained by the mean growing season VPD in the species' native ranges: WUE was correlated with native VPD across all species (Figure 2.5), showing that species originating from climates with dry atmospheres, such as Australia, are adapted to grow quickly relative to the amount of water used in transpiration. Hence, although Australian species such as *Eucalyptus* have a reputation for high water use, they are actually quite efficient given their rapid rate of growth.

Figure 2.4: Basal Area Increment (BAI) vs. transpiration of Los Angeles tree species



Source: McCarthy et al. (2011)

Figure 2.5: Water Use Efficiency (WUE) versus growing season precipitation and Vapor Pressure Deficit in species native environment



Source: McCarthy et al. (2011)

2.1.2 Database of plant transpiration

Transpiration varies both in space and time due to species specific differences in water use, climatic variability, and local site conditions. Because transpiration rates are highly sensitive to climate, average E_w is insufficient to predict transpiration under a particular set of environmental conditions. Instead, it is useful to model E_w as a function of variability in VPD and I_o , the main environmental drivers of transpiration under well-watered conditions. Where soil moisture is limiting due to irregular or insufficient irrigation, the response of E_w to soil moisture must also be taken into account (McCarthy and Pataki 2010). Therefore, we developed our transpiration database as a set of response functions of E_w to VPD , I_o , and soil moisture

rather than merely reporting average E_w over time. This will greatly expand its potential use in predicting urban plant transpiration.

During our field campaigns, we measured temperature and relative humidity in the canopy (HMP45C, Vaisala Inc., Helsinki, Finland), and used these values to calculate VPD . We measured overstory incident radiation (I_o) where logistically possible, and used data from California Irrigation Management Information System weather stations (<http://CIMIS.water.ca.gov>) within a 20 km distance from our study sites as a reliable substitute. We also measured soil water content at 6 locations at each study site except for one (it was not feasible to measure soil moisture near the street trees). Soil water content reflectometers (CS616, Campbell Scientific, Logan, Utah) were inserted in the top 30 cm of the soil, and relative water content (Θ) determined by dividing the measured soil water content by the maximum value recorded at each location. We used Θ to quantify the relative response of J_o to changing soil moisture (Pataki & Oren 2003). Temperature, relative humidity, I_o and soil water content were sampled every 30 seconds, and stored as 30-minute averages by the dataloggers (CR10X, CR1000, and CR3000, Campbell Scientific Inc., Logan, UT, USA).

We evaluated responses of E_w to VPD within canopies averaged over daylight hours, the daily sum of I_o and Θ as an empirical model:

$$E_w = y_0 + a \ln(VPD) + b(I_o) + c \Theta \quad (2.5)$$

Mean model coefficients y_0 , a , b , and c and their standard error are listed in Table 2 when statistically significant at $\alpha = 0.05$. When a model parameter was insignificant, we excluded it from the equation and obtained the best fit with the remaining parameters. On one occasion VPD was not correlated with E_w : *P. canariensis* in Los Angeles Police Academy, the trees in which the model explained the least variability in E_w ($R^2 = 0.24 \pm 0.11$). The most variability ($R^2 = 0.83 \pm 0.04$) was obtained for *Platanus racemosa* at the Los Angeles residential street. Most model coefficients were positive, with negative b for *Jacaranda* species only, and negative c for *J. chelonina* and *S. sempervirens* at the University of California, Irvine campus.

Table 2.3: Coefficients of the model described in equation (2.5).

Species	Site	Year(s)	Days of study	No. trees	E_w (kg day ⁻¹ tree ⁻¹)	y_0	a	b	c	adj. R ²
<i>Brachychiton discolor</i>	LAA	2008-2009	81-30	12	23.0 ± 10.5	12.1 ± 2.7	12.9 ± 2.0	0.1 ± 0.1	20.2 ± 3.5	0.46 ± 0.04
<i>Brachychiton populneus</i>	LAA	2008-2009	81-30	7	13.8 ± 8.5	6.0 ± 3.1	7.5 ± 1.4	0.1 ± 0.1	7.5 ± 2.0	0.49 ± 0.06
<i>Eucalyptus grandis</i>	LAA	2008-2009	81-30	4	53.7 ± 24.1	31.7 ± 22.7	21.3 ± 5.2	0.3 ± 0.7	45.3 ± 7.6	0.58 ± 0.03
<i>Eucalyptus grandis</i>	UCI	2008-2009	106-48	6	13.3 ± 10.6	11.2 ± 4.8	6.1 ± 2.2	0.1 ± 0.1	5.4 ± 3.5	0.36 ± 0.09
<i>Ficus microcarpa</i>	LAS	2008-2009	98-21	4	102.7 ± 18.6	122.0 ± 1.9	33.8 ± 9.5	0.7 ± 0.9	58.4 ± 13.8	0.46 ± 0.01
<i>Gleditsia triacanthos</i>	LAS	2008	98-324	3	93.7 ± 26.2	89.3 ± 27.6	29.0 ± 7.2	0.8 ± 0.7	-	0.36 ± 0.04
<i>Jacaranda chelonina</i>	LAS	2008-2009	98-29	3	83.3 ± 24.0	70.8 ± 27.6	43.0 ± 18.5	-0.1 ± 0.4	-20.7 ± 3.6	0.54 ± 0.04
<i>Jacaranda mimosifolia</i>	LAZ	2007-2008	180-22	6	10.9 ± 5.6	10.2 ± 3.5	5.5 ± 1.4	-0.3 ± 0.1	8.4 ± 4.6	0.42 ± 0.06
<i>Koeleruteria paniculata</i>	LAS	2008	98-324	4	71.3 ± 33.8	41.5 ± 17.5	20.5 ± 1.8	1.1 ± 0.4	10.0 ± 15.0	0.55 ± 0.06
<i>Lagerstroemia indica</i>	LAS	2008	98-324	6	46.9 ± 11.0	11.5 ± 1.9	10.3 ± 1.6	0.7 ± 0.1	26.9 ± 2.8	0.60 ± 0.05
<i>Pinus canariensis</i>	LAZ	2007-2008	180-22	7	14.7 ± 4.5	23.5 ± 5.4	11.5 ± 2.6	-	-	0.33 ± 0.10
<i>Pinus canariensis</i>	PA	2008-2009	69-22	5	37.8 ± 13.1	18.2 ± 2.2	-	0.6 ± 0.4	10.2 ± 1.7	0.24 ± 0.11
<i>Pinus canariensis</i>	UCI	2007-2008	200-31	5	50.0 ± 7.9	13.4 ± 2.5	8.9 ± 1.6	1.0 ± 0.1	24.0 ± 4.9	0.69 ± 0.05
<i>Platanus hybrida</i>	SS	2007-2008	125-34	4	91.5 ± 37.0	32.8 ± 18.3	49.9 ± 10.0	2.9 ± 1.1	no data	0.70 ± 0.07
<i>Platanus racemosa</i>	SS	2007-2008	125-34	3	64.7 ± 11.0	38.9 ± 8.1	34.2 ± 3.9	1.2 ± 0.1	no data	0.83 ± 0.04
<i>Platanus racemosa</i>	STR	2007-2008	174-4	8	23.3 ± 11.3	-26.0 ± 4.8	8.6 ± 1.8	-	57.4 ± 12.7	0.62 ± 0.04
<i>Platanus racemosa</i>	UCI	2007-2008	200-31	5	29.6 ± 13.5	23.9 ± 4.1	25.1 ± 8.1	0.8 ± 0.3	-	0.60 ± 0.10
<i>Quercus agrifolia</i>	STR	2007-2008	174-4	7	8.7 ± 5.7	6.8 ± 2.4	3.8 ± 0.8	-	0.2 ± 6.0	0.37 ± 0.05
<i>Sequoia sempervirens</i>	FUL	2008-2009	129-18	9	25.7 ± 11.9	10.1 ± 3.2	6.9 ± 1.5	0.4 ± 0.1	4.2 ± 2.3	0.79 ± 0.01
<i>Sequoia sempervirens</i>	PA	2008-2009	69-22	5	10.9 ± 5.8	0.4 ± 2.6	2.8 ± 0.8	0.3 ± 0.1	4.2 ± 1.3	0.50 ± 0.02
<i>Sequoia sempervirens</i>	UCI	2008-2009	106-48	8	20.3 ± 8.3	10.6 ± 2.9	3.2 ± 0.6	0.3 ± 0.1	-5.1 ± 2.0	0.69 ± 0.02
<i>Ulmus parvifolia</i>	PA	2008-2009	69-22	5	47.1 ± 13.0	11.7 ± 7.6	10.7 ± 1.8	1.2 ± 0.3	-	0.62 ± 0.04

2.2 Plot-level transpiration

We utilized our measurements of transpiration to estimate the water use of whole landscapes at the plot level. This was the first time that direct measurements of urban forest water use have been available at this spatial scale. We conducted two scaling studies to estimate plot level water use, one for forest plots that considered trees but no other vegetation, and one that considered mixed plots of trees and lawns. While lawn ET has been estimated previously,

estimates for mixed plots in which lawns are planted with other types of vegetation have not previously been published. Because the density of trees and other vegetation varies greatly in urban landscapes, we expressed plot level transpiration as a function of tree density and cover.

2.2.1 Urban forest transpiration

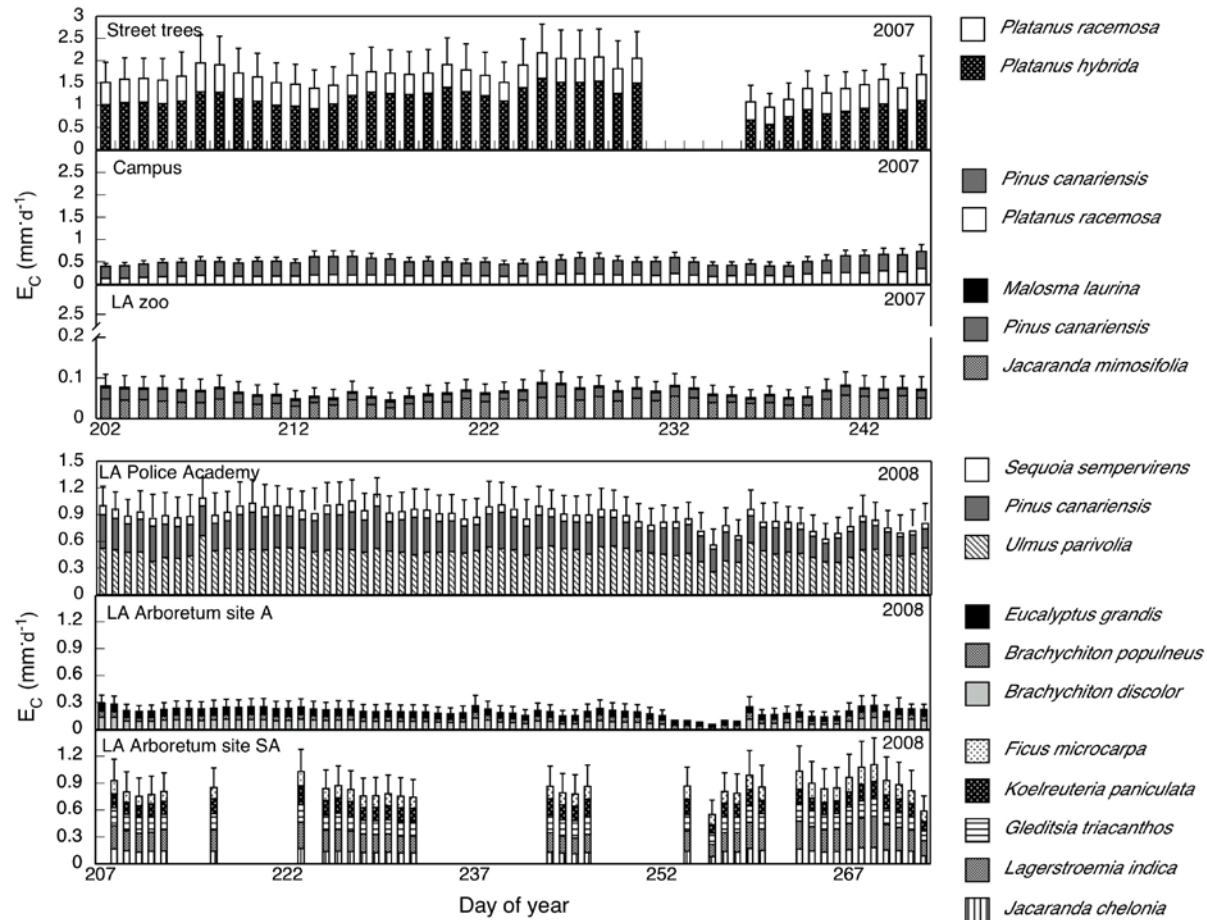
We estimated plot-level canopy transpiration (E_c , $\text{mm}\cdot\text{d}^{-1}$) at our sap flux measurement sites by summing E_w for all measurement trees and dividing by the plot area. The error of each estimate was generated by propagating the variance in sap flux rates among individuals of each species with the error of the algorithm used to specify radial trends from equations (2.2) and (2.3). To estimate the error at each 2 cm sapwood increment (Δ) we used the equation:

$$\sigma_i = J_i \sqrt{\left(\frac{\sigma_o}{J_o}\right)^2 + \left(\frac{\sigma_R}{J_i : J_o}\right)^2} \quad (2.6)$$

where J_o is sap flux in the outer 2 cm of xylem, σ_o is the standard deviation in J_o , and σ_R is the error of the radial trends regression estimate. The error in each sapwood increment was then propagated to estimate the total error.

E_c for each plot that we studied and the proportional contribution of each species is shown in Figure 2.6. The Los Angeles Street tree site showed the highest E_c , with values exceeding $2 \text{ mm}\cdot\text{d}^{-1}$. However, plot areas are difficult to determine for urban landscapes and for street trees in particular. In a relatively uniform forest similar to natural forests, the specification of plot area is not important – transpiration is assumed to be homogenous and plot areas may be (and should be) determined randomly. However, in urban landscapes there is a highly heterogeneous mix of pervious soils and impervious surfaces. The plot area of sidewalk trees may be defined in many ways – by the pervious soil area (which is very small and would result in very high estimates of E_c), the entire sidewalk area, the sidewalk plus the road area, and so forth. For the street tree site, if only pervious surfaces are included in the determination of plot area, E_c would be more than four times higher, with values exceeding $9 \text{ mm}\cdot\text{d}^{-1}$. As far as the contributions of each species to total E_c , *Platanus hybrida* (London planetree) was a larger contributor to E_c than *P. racemosa* (California sycamore) at the street tree site, due both to higher sap flux rates and greater tree size and number in *P. hybrida*. At the Los Angeles Zoo, irrigated *Jacaranda mimosifolia* contributed the majority of E_c (Figure 2.6). E_c was also relatively high at the Los Angeles Police Academy, with values ranging from $0.5 - 1.0 \text{ mm}\cdot\text{d}^{-1}$ (Figure 2.6). *Ulmus parvifolia* and *Pinus canariensis* constituted the majority of E_c at this site, with very small contributions from *Sequoia sempervirens* (Figure 2.6). There were relatively equal contributions to E_c by species at the Arboretum sites (Figure 2.6).

Figure 2.6: Plot-level urban forest canopy transpiration (E_c) by species and site

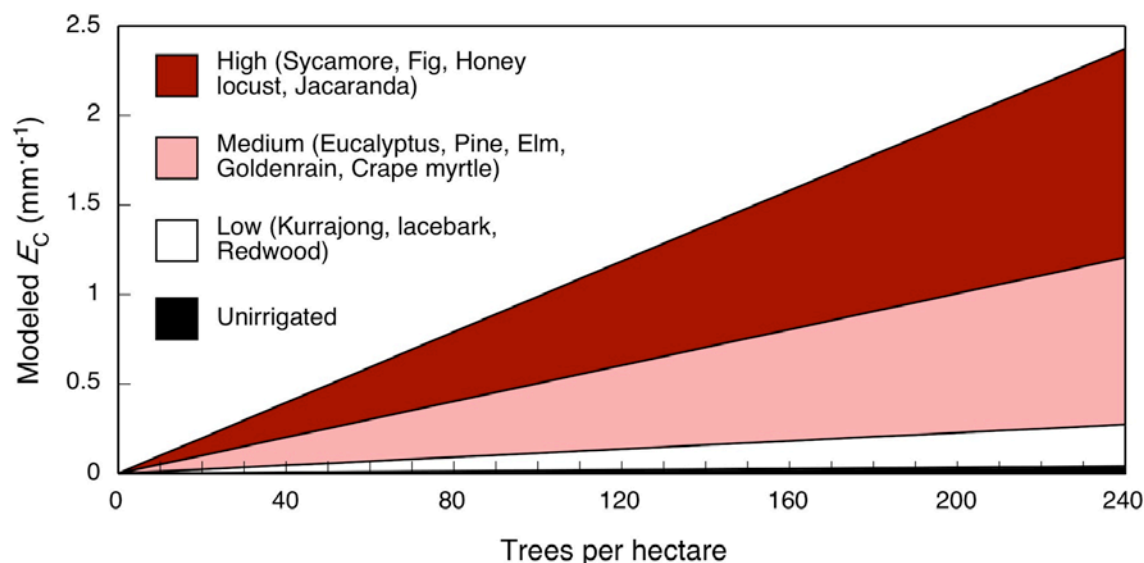


Source: Pataki et al. (2011)

To make our results more applicable to a large range of urban forest sites, we expressed E_c as a function of tree density, so that E_c may be estimated for areas with sparse as well as relatively densely planted trees. We also categorized each species as low, medium, or high water users when well-irrigated to assess the influence of species selection on forest level transpiration. At the highest tree density that we measured of 240 trees per hectare (which is still relatively low compared to natural forests) plot level forest transpiration was strongly influenced by species. In fact, forest transpiration varied by a factor of 10 for low transpiring vs. high transpiring species, even when well-irrigated (Figure 2.7). Redwoods and Australian *Brachychiton* species, for example, have very low rates of canopy transpiration, even when the soil is very moist, relative to commonly planted sycamore, ficus, and jacaranda. Hence, the choice of landscape tree species has a very large influence on total forest transpiration – much higher than has previously been discussed due to the lack of direct measurements of the transpiration rates of urban trees. Our measurements show that species selection may make the difference between E_c of 0.2 mm/day vs. 2 mm/day, which is an enormous range of possible transpiration rates. Furthermore, our results show that previous assumptions about the suitability of various species for water conservation are not always supported by direct measurements. Some species

previously assumed to have high transpiration rates, such as Eucalyptus, are moderate water users, while others, such as the native California sycamore, have very high rates of transpiration.

Figure 2.7: Plot-level urban forest canopy transpiration (EC) modeled as a function of tree density and species



Source: Pataki et al. (2011)

2.2.2 Transpiration of lawns and mixed vegetation cover

We also assessed water use of non-forested and mixed grass-tree plots. Turfgrass ET is estimated by the California Irrigation Management Information System (<http://www.cimis.water.ca.gov>) with a modified Penman equation (CIMIS equation) and an empirical crop coefficient for turf. We measured the meteorological variables necessary for utilizing the CIMIS equation, and we also made direct measurements of turfgrass ET with a static chamber for comparison. We then estimated plot-level ET for both turfgrass plots and for mixed tree-grass plots at three locations in the Los Angeles Basin: the UC Irvine campus, Fullerton Arboretum at the Cal State Fullerton campus, and the Los Angeles County Arboretum and Botanical Garden.

At each site we chose a turfgrass lawn and a mixed tree-grass landscape. At each of these plots we measured incoming shortwave radiation (I_0) with Apogee pyranometers (Apogee Inc, Logan, Utah) connected to hand-held digital voltmeters and temperature (T_a) and atmospheric relative humidity with HOBO Pro V2 dataloggers (Onset Computer Corporation, Bourne, MA) at 1 m above the ground. We estimated daily I_0 and mean VPD during daylight hours by fitting Gaussian functions to diurnal profiles of these variables:

$$y = a \exp \left[-\frac{1}{2} \left(\frac{t - t_0}{b} \right)^2 \right] \quad (2.7)$$

followed by analytical integration:

$$a \int_{-\infty}^{+\infty} \exp \left[-\frac{1}{2} \left(\frac{t - t_0}{b} \right)^2 \right] \cdot dt = ab\sqrt{2\pi} \quad (2.8)$$

We also measured soil water content (Θ) at 0-5 cm depth using portable sensors (ML2x Theta Probe with HH2 moisture meter, Delta-T Devices LTD, Cambridge, UK and HydroSense Soil Water Measurement System, Campbell Scientific Inc., Logan, Utah, USA). We made 4-6 measurements of Θ per day in June, but since soil moisture remained stable over the course of the day, we later reduced frequency to 1-3 measurements a day. To quantify net radiation (R_N), we chose a spot with a 10 m footprint of irrigated turfgrass at each location and mounted a net radiometer (CNR1, Kipp & Zonen, Delft, Netherlands) on a portable tripod stand (T-1000, Columbia Weather Systems, Hillsboro, Oregon, USA) at 1m height. We measured R_N and its components at each location, derived linear relationships between I_o and R_N for each location, and used this relationship to estimate R_N from diurnal patterns of I_o . To measure the ground heat flux (G), we installed 5 soil heat-flux plates (HFPO1, Huxeflux Thermal Sensors B.V., Delft, Netherlands) at 5 cm depth for one day in June at each study site. The data from net radiometer and soil heat-flux plates were logged every 30 s and averaged every 15 min by dataloggers (CR1000 and CR3000, Campbell Scientific Inc., Logan, Utah).

For the chamber ET measurements, we used clear PVC chambers 0.18 m high and 0.28 m wide (McLeod et al. 2004). Air temperature and humidity inside the chambers was recorded by HOBO Pro V2 wireless dataloggers (Onset Computer Corporation, Bourne, MA, USA) every 2 seconds. At 6 sampling spots at each study site, we made 3-6 chamber measurements per day in summer and 5-9 measurements per day in winter, coinciding with the measurements of I_o and VPD. During each measurement, a chamber was tightly pressed on the grass surface for 1 minute. Between measurements, the chambers were ventilated for at least 1 minute with ambient air. We calculated the mass density of water vapor inside the chamber (ρ_v , kg/m³) using the ideal gas law:

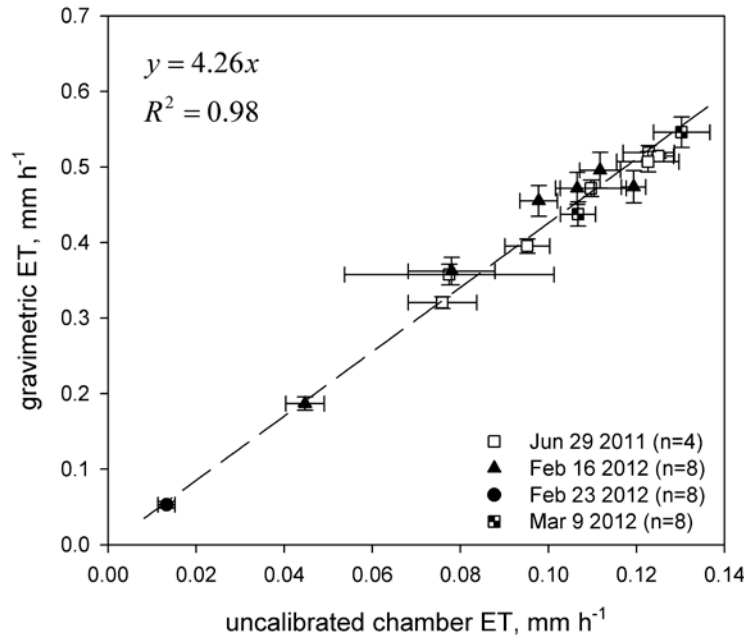
$$\rho_v = \frac{e}{R_v(273.15 + T)}, \quad (2.9)$$

where e is the vapor pressure inside the chamber in Pa, $R_v = 461.5 \text{ J K}^{-1} \text{ kg}^{-1}$ is the gas constant for water vapor, and T is the temperature inside the chamber in °C. The increase of ρ_v caused by ET ($d\rho_v/dt$) was obtained as a slope of ρ_v versus time for stable periods of 10-30 s. ET (m³H₂O m⁻² s⁻¹) was calculated from chamber measurements as

$$ET_{ch} = k \frac{h}{\rho_w} \frac{d\rho_v}{dt}, \quad (2.10)$$

where h is the height of the chamber (0.18 m), $\rho_w = 10^3 \text{ kg m}^{-3}$ is the mass density of water, and k is the calibration factor discussed below.

Figure 2.8: ET measured gravimetrically with weighing lysimeters vs. chambers



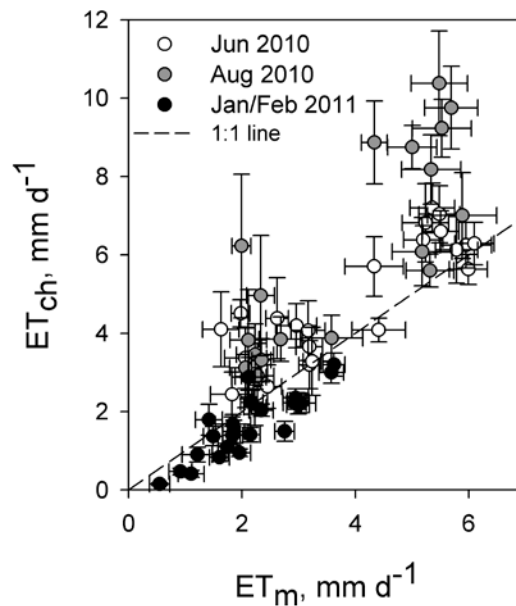
Source: Litvak et al. (In review)

There are known artifacts of utilizing static chambers for measuring ET, including shielding of near-surface winds and absorption of water vapor by chamber walls (McLeod et al. 2004), as well as effects of slow sensor response times. Therefore, we calibrated the chambers with weighing lysimeter measurements in the lab. We used 4 to 8 [0.22cm×0.22cm] well-watered sod samples of tall fescue and Bermuda grass in metal mesh frames that were sealed with plastic on the sides and below to avoid leakage. We weighed the samples (OHAUS AdventurerPro AV 3102 balance, OHAUS Corporation, Parsippany, NJ, USA) in the laboratory and made chamber measurements of each sample outside at the campus of UC Irvine. We made these measurements repeatedly for several hours each day, at the beginning and the end of each hour. The samples were covered by a chamber for a total of 2 min each hour, and spent the other 2 min per hour inside for weighing. We plotted mean chamber ET for each hour against balance readings that reflected integrated water losses per hour. The resulting calibration factor $k = 4.26 \pm 0.05$ (Fig. 2.8) was then applied to the ET_{ch} calculation (Eq. 10). We fitted Gaussian functions to diurnal ET_{ch} patterns, and calculated daily ET_{ch} using analytical integration similar to I_o and D (Eq. 2.7 and 2.8).

Calibrated chamber ET (ET_{ch}) agreed fairly well with CIMIS ET (ET_m), except during the summer (Figure 2.9). In particular, at the Fullerton site in August, ET_c was much higher than

ET_m . Both methods have limitations so it is not straightforward to say which method, if any, is closer to estimating actual ET. Crop coefficients are entirely empirical and do not account for the many factors that can influence stomatal and canopy conductance at a particular location, such as species composition, soil types, and other site factors. On the other hand, static chambers poorly account for variable wind conditions, and the calibration factor that we obtained with lysimeters may neglect other important site factors.

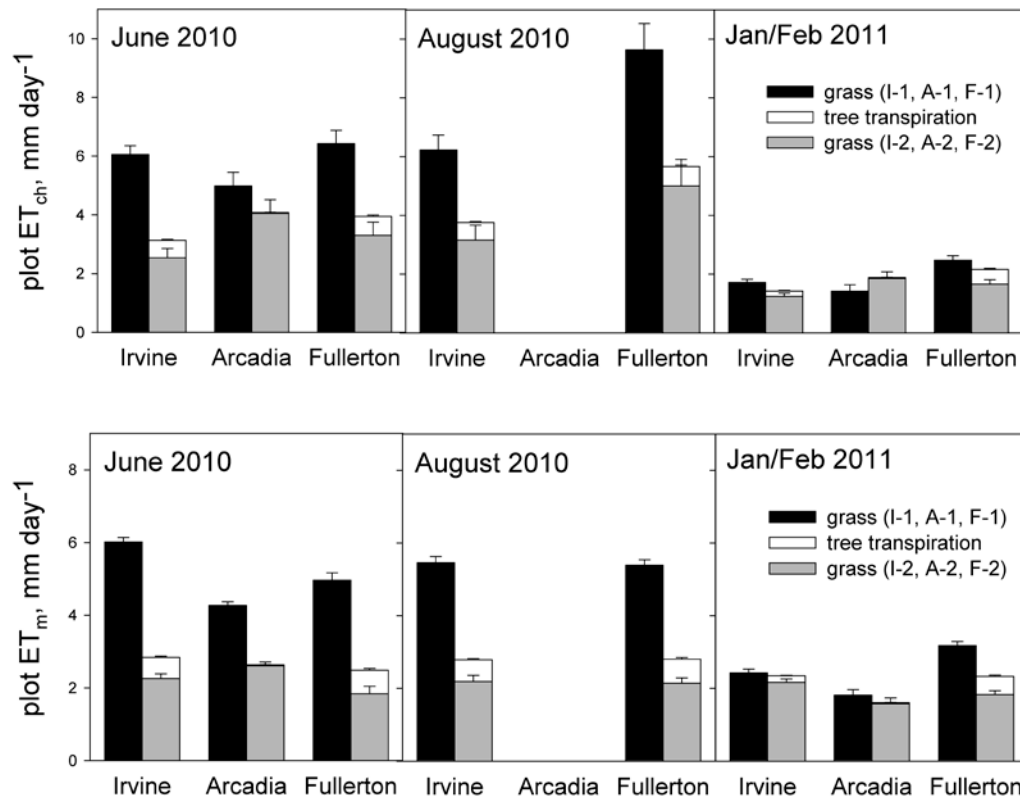
Figure 2.9: ET measured with chambers (ET_{ch}) vs. modeled ET (ET_m) from CIMIS



Source: Litvak et al. (In review)

Nevertheless, both methods agreed when assessing the influence of trees on turfgrass ET. For the plots that contained trees, we utilized the transpiration database in Table 2.2 to model tree transpiration as a function of meteorological variables. We also measured the total Leaf Area Index (LAI) of the lawns through destructive harvest to estimate total turfgrass ET of the plot. Using this method, we estimated plot ET for (1) ET of 100 percent turfgrass lawns, shown in solid bars in Figure 2.10) ET of mixed turfgrass and tree landscapes, shown in grey and white bars in Figure 2.10. Both the chamber method and CIMIS modeled ET showed the same pattern: ET of mixed tree-grass landscapes was lower than pure turfgrass lawns. This is due both to shading effects of trees, and also because trees have lower transpiration rates per unit leaf than turfgrass. Hence, while it may seem counterintuitive, adding trees to turfgrass landscapes may actually reduce water consumption relative to areas of continuous, unshaded lawns.

Figure 2.10: ET of 100% turfgrass plots (black bars) and mixed tree-lawn plots (grey and white bars)



Source: Litvak et al. (In review)

2.2.3 Lawn water budgets

Finally, we utilized the chamber method and along with measurements of irrigation inputs, surface runoff, and drainage to determine the complete water budget for three experimental lawns at the South Coast Research and Extension Center in Irvine, CA. This is a UC Davis run facility that conducts agricultural and horticultural experiments. In 2006, Dr. Darren Haver established an experiment to evaluate the environmental impact of residential front and backyards that utilize different management practices. This experiment is still ongoing; there are three treatments: 1) The “typical” yard contains a fescue lawn (*Schedonorus phoenix*) and is watered with an automated irrigation timer that waters daily in the summer months. The lawn is surrounded by impervious pavement. 2) The “retrofitted” yard utilizes improvements that a homeowner might make to retrofit a typical yard: the lawn contains the warm season grass species seashore paspalum (*Paspalum vaginatum*) watered with a soil-moisture based irrigation system, and the driveway adjacent to the lawn was retrofitted with permeable pavers. 3) The “low-impact” yard was designed with state-of-the-art Low Impact Development (LID) features, including a native California sedge lawn species (*Carex* spp.), an irrigation system tied to the CIMIS network that waters at the recommended rate based on local weather, and paved surfaces that are completely permeable.

This experiment is instrumented with equipment for measuring and sampling runoff from each yard (a water sensing sump pump and flow meter). We added additional instrumentation to estimate the complete water budget for the lawn portion of each yard including soil moisture sensors (CS 616, Campbell Scientific, Inc., Logan, UT, USA), periodic measurements of ET with the chamber method described above, measurements of leaf stomatal conductance with a porometer (SC-1, Decagon Devices, Pullman, WA), and containers for measuring the amount of irrigation water applied to each lawn. We estimated ET in two ways: using chamber method and also by applied our measured values for stomatal conductance to a modified Penman-Monteith equation based on Allen (1998):

$$\lambda ET = \frac{\Delta(R_n - G) + \rho_a c_p \frac{VPD}{r_a}}{\Delta + \gamma(1 + \frac{g_a}{g_s})} \quad (2.11)$$

where R_n is the net radiation measured at the nearby CIMIS station 0.3 km from the sites (www.cimis.water.ca.gov, Irvine station #75), G is the soil heat flux, calculated as 10 percent of R_n (Allen, 1998), ρ_a is the mean air density at constant pressure, c_p is the specific heat of air, Δ is the slope of the saturation vapor pressure temperature relationship, γ is the psychrometric constant, and g_a and g_s are the aerodynamic and canopy conductances.

The aerodynamic conductance (g_a) was calculated as

$$g_a = \frac{k^2 u_z}{\ln \frac{z_m - d}{z_{om}} \ln \frac{z_h - d}{z_{oh}}} \quad (2.12)$$

where k von Karman's constant, u_z is wind speed measured at the nearby CIMIS station, z_m is the height of wind measurements (2 m), z_h is height of humidity measurements (2 m), and d is the zero plane displacement height:

$$d = \frac{2}{3} * h \quad (2.13)$$

where h is crop height: 0.076 m and 0.025 m for fescue and paspalum, respectively, and 0.12 m for sedge.

We estimated z_{om} , the roughness length governing momentum transfer, as:

$$z_{om} = 0.123 * h \quad (2.14)$$

We estimated z_{oh} , the roughness length governing transfer of heat and vapor, as:

$$z_{oh} = 0.1 * z_{om} \quad (2.15)$$

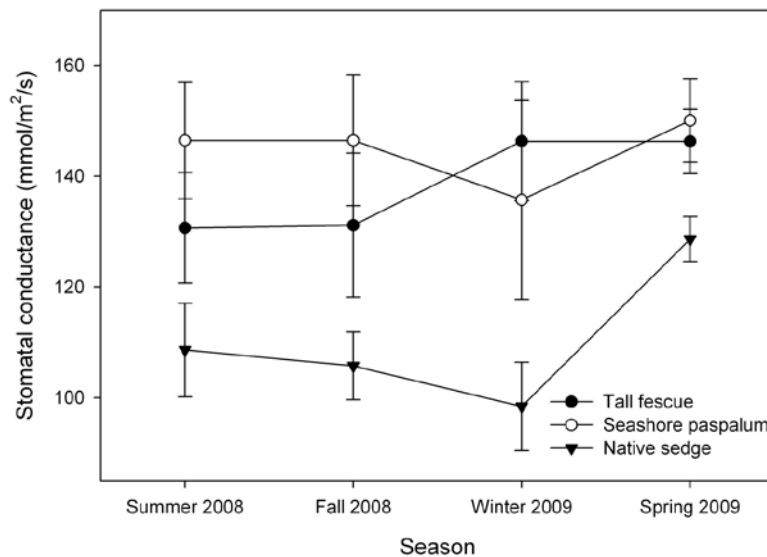
Canopy conductance (g_s) was calculated as:

$$g_s = g_l * LAI_{active} \quad (2.16)$$

where g_i is measured leaf stomatal conductance, which was directly measured. LAI_{active} , or the Leaf Area Index of actively transpiring leaves, was determined as:

$$LAI_{active} = 0.5 * 24 * h \quad (2.17)$$

Figure 2.11: Leaf stomatal conductance measured in the three lawns



Source: Bijoor et al. (In review)

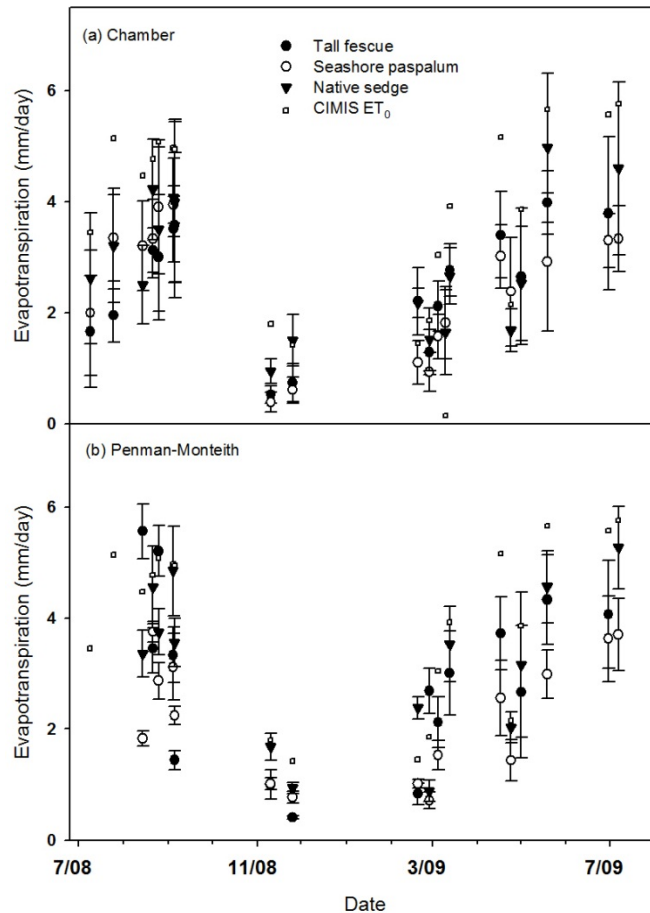
Similar to our findings for tree transpiration, we found that g_i was species specific, with the native sedge species showing lower g_i than the other two lawn species (Figure 2.11). However, the sedge lawn had a higher LAI than the other two lawns, such that ET was similar among the three lawns (Figure 2.12). ET measured by the chamber method and estimated from the Penman-Monteith based model were similar; however, both methods yield lower estimates of ET than the Reference ET values calculated by CIMIS (Figure 2.12).

We constructed complete water budgets for the three lawns using both chamber and Penman-Monteith based estimates of ET. Both yielded similar results (Figure 2.13). The typical lawn resulted in the highest irrigation rates and the lowest proportion of irrigation allocated to ET. More than half of the ET applied to the typical lawn was lost as drainage below the rooting zone (Figure 2.13). Surface runoff was small to negligible in all three lawns; this is likely a function of soil texture, as soils at this particular site were sandy. In soils containing a higher clay content, it is likely that a higher percentage of irrigation water would be lost as runoff rather than drainage.

The most water efficient lawn was not actually the low impact lawn, but the retrofitted lawn, which contained a commercially available irrigation system that triggered watering during conditions of low soil moisture, based on direct soil moisture measurements. This system

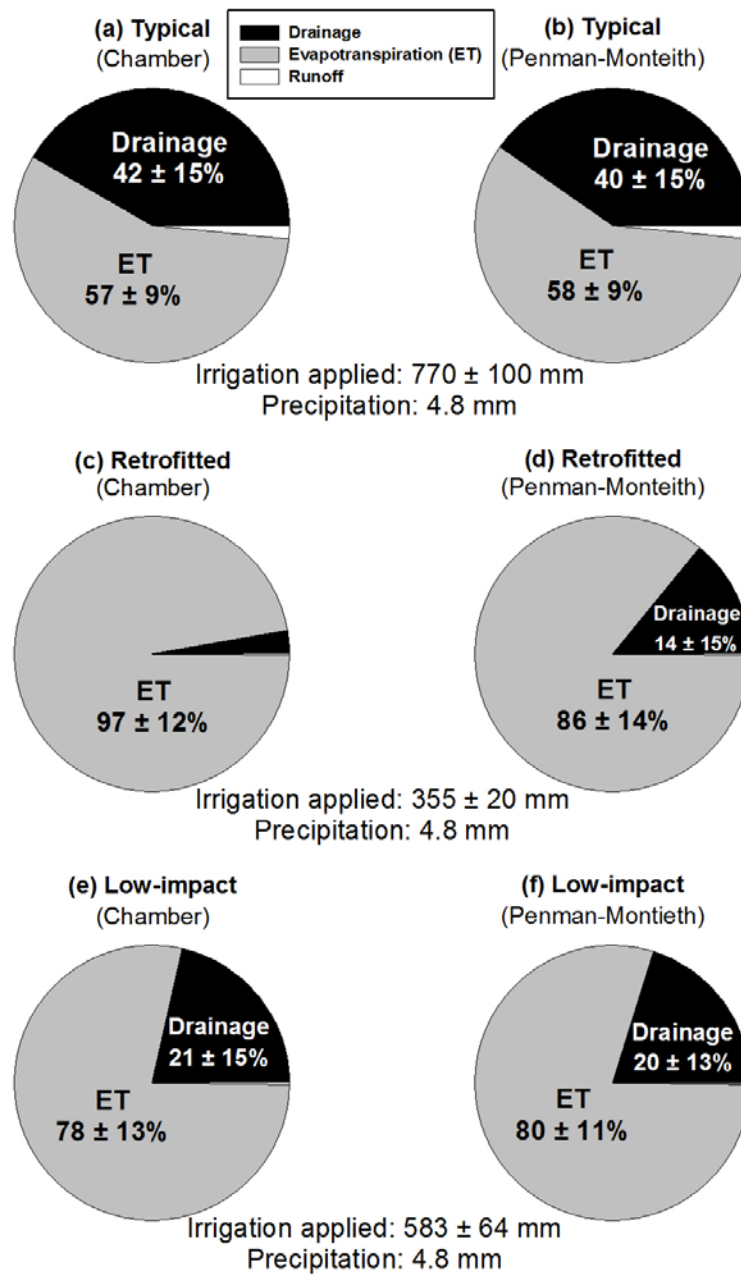
applied the least amount of water, and the vast majority was used as ET rather than lost as drainage or runoff (Figure 2.13). The low impact lawn utilized a weather station-based irrigation system tied to the CIMIS network. However, our results suggests that CIMIS currently over-estimates lawn ET (Figure 2.12); estimates of reference ET could be improved by incorporating measurements of stomatal conductance and LAI by lawn type. These are relatively simple measurements and a database of stomatal conductance and LAI for common lawn types and management practices may fine tune estimates of the water requirement of lawns in California.

Figure 2.12: Evapotranspiration of the three lawn types estimated with the chamber method (upper panel) and Penman-Monteith modeling based on direct measurements of stomatal conductance and LAI (lower panel) compared to reference ET calculated by CIMIS



Source: Bijoor et al. (In review)

Figure 2.13: Complete water budgets for the three experimental lawns using both chamber-based and Penman-Monteith based estimates of ET.



Source: Bijoor et al. (In review)

CHAPTER 3:

Remote Sensing and Ground-based Evapotranspiration Models for Los Angeles

3.1 Remote Sensing Model

3.1.1 UCLA-ET Algorithm

Previous work by the Hogue research group at UCLA resulted in the development of a range of remote sensing data-based models to estimate Potential Evapotranspiration (PET) and actual Evapotranspiration (ET) (Kim and Hogue, 2008; 2012a; 2012b). These models are very useful in that remote sensing data is available for urban areas and can capture the high degree of spatial variability in energy balance parameter that is a feature of most cities. The most recent UCLA-ET model is based on a remote sensing algorithm developed to retrieve ET at a daily time step and 30m spatial resolution. The method evaluates the components of the energy balance and determines the ET rate as a residual by adapting the Surface Energy Balance Algorithm for Land (SEBAL) model (Bastiaannssen et al., 1998). The uniqueness of the UCLA-ET model is the computation of the energy balance parameters (i.e., Net radiation, Soil Heat flux and Sensible Heat Flux) that come primarily from remote sensing products and involves the merging of spatial detail of higher resolution imagery (i.e., Landsat) with the temporal change observed in coarser or moderate resolution imagery (i.e., MODIS). The resulting merged images allows us to retrieve ET at both a high temporal (i.e., daily) and spatial (i.e., 30m) resolution. In the SEBAL model, LE (or ET) is calculated as the residual of the energy balance equation:

$$LE = R_n - G - H \quad (3.1)$$

where R_n is the net radiation, G is soil heat flux and H is the sensible heat flux. Net radiation comprises two major components, net shortwave and longwave radiation.

$$R_{n,LM} = (1 - \alpha_{LM})S_d + L_d - L_u \quad (3.2a)$$

$$= (1 - \alpha_{LM})S_d + \varepsilon_{LM}\varepsilon_a\sigma T_a^4 - \varepsilon_{LM}\sigma T_{rad,LM}^4 \quad (3.2b)$$

where S_d is downward shortwave radiation, L_d is downward longwave radiation, L_u is upward longwave radiation. σ is the Stefan-Boltzmann constant ($5.67 \times 10^{-8} \text{ W/m}^2 \text{ K}^4$), α is surface albedo and ε and ε_a is surface emissivity and air emissivity, respectively. T_a is air temperature, T_{rad} is surface radiative temperature.

Soil heat flux (G) is derived from net radiation (R_n), surface temperature (T_{rad}), Normalized Difference of Vegetation Index (NDVI) and albedo(α) using:

$$G = R_n(T_{rad} - 273)(0.0038 + 0.0074\alpha)(1 - 0.98NDVI^4) \quad (3.3)$$

The core component of the SEBAL ET approach is the H scheme calculated through:

$$H = \rho C_p \frac{dT}{r_{ah}} = \rho C_p \frac{aT_{rad} + b}{r_{ah}} \quad (3.4)$$

where ρ is the air density; C_p is the specific heat of air at constant pressure; r_{ah} is aerodynamic resistance; dT is the difference between aerodynamic temperature and air temperature, which assumed linearly related (a and b are coefficients of a linear relationship derived from hot/cold pixel extremes). One of the key issues with the SEBAL method is the appropriate selection of the extreme hot and cold pixels used in derivation of the sensible heat flux. Particularly, urban environments may not consist of the necessary three spectral endmembers of fully vegetation (irrigated), dry bare soil, open-water surface from pure (unmixed) pixels. As in Johnson and Belitz (2012), we select two golf courses/parks (i.e., Beverly hills golf course and Los Amigos golf course) as the irrigated-landscaping endmember. For the bare soil endmember, two local barren areas were delineated. A third endmember (water-body) was also identified in two local lakes and reservoirs (i.e., Silver Lake, Hollywood reservoir).

The r_{ah} variable is aerodynamic resistance between two heights (generally 0.1 and 2m above the surface) computed as a function of aerodynamic roughness through equation (9)-(11).

$$r_{ah} = \log\left(\frac{2}{0.1}\right) / (0.41 u^*) \quad (3.5)$$

$$u^* = 0.41 u_{200} / \log\left(\frac{200}{Z_m}\right) \quad (3.6)$$

$$u_{200} = u \frac{\log\left(\frac{200}{Z_m}\right)}{\log\left(\frac{2}{Z_m}\right)} \quad (3.7)$$

where u^* is the friction velocity (m/s), u_{200} and u are the wind speed at 200m and 2m (m/s), respectively. u is obtained from ground based observation. In this study, we obtained the wind data from the Glendale CIMIS station and the roughness length (Z_m) is retrieved from standard parameters based on land cover types.

Given H , R_{net} and G at the instant of the satellite image, the instantaneous evaporative fraction (EF_{inst}) can be directly estimated through equation (3.8).

$$EF_{inst} = 1 - \frac{H}{R_{net} - G} \quad (3.8)$$

For cloudy days, we use the temporal interpolation method proposed by Jiang et al., 2009 to fill the EF based on the assumptions that the EF is consistent between clear and cloudy days (Tasumi et al., 2005). First, all EF values for cloudy days are filled by neighboring clear days in time series. After this gap filling, two smoothing processes are performed: 1) 5-days median

filtering and 2) 15-day statistical smoothing. These processes remove extremely high and low values of EF and abrupt changes between days.

3.1.2 Remote Sensing Data

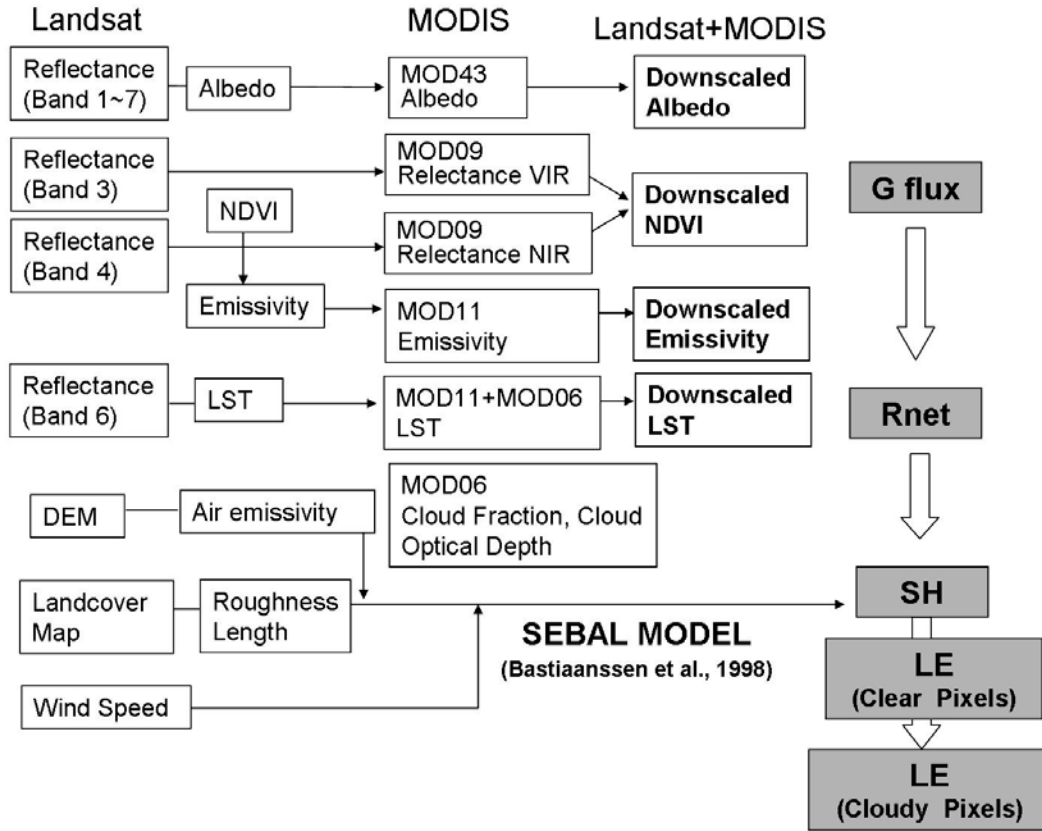
Remotely sensed data used in the above algorithm include Moderate Resolution Imaging Spectroradiometer (MODIS) sensors on board the Aqua and Terra platforms, which include 36 bands and higher radiometric resolution than previous sensors such as AVHRR which had five bands. Terra data are available 2000 to present (March 2007, at least). We integrate (at least) the following sensors: MOD03, MOD04, MOD05, MOD06, MOD11, MOD13, MOD43.

Landsat5 TM (bands 2,3,4,6 and 7). The TM bands 1-5 and 7 provide reflectance data for the visible and near infrared radiation at 30m spatial resolution. TM band 6 measures thermal radiation at 120m and has been resampled at 60m (data processed before 02/2010) and at 30m (data processed after 02/2010).

Table 3.1: MODIS and Landsat satellite products and their spatial and temporal resolution used in the SEBAL-based UCLA-ET algorithm.

MODIS (Terra/Aqua)				Landsat5		
Product Name	Variable	Pixel (grid) resolution	Temporal resolution	Band	Pixel (grid) resolution	Temporal resolution
MOD(MYD) 03	Zenith Angle, Geolocation	1 x1km	Daily	-	-	-
MOD(MYD) 05	Water Vapor	1 x1km	Daily	-	-	-
MOD(MYD) 06	LST, Emissivity of Cloud, Cloud Top LST, Cloud Optical Depth, Cloud Fraction	1 x1km 5 x5km	Daily	-	-	-
MOD(MYD) 07	Air Temperature, Dew Point Temp.	5 x5km	Daily	-	-	-
MOD(MYD) 11	LST, Emissivity	1 x1km	Daily	3,4,6	30m, 60m	16-day
MOD(MYD) 13Q1	Vegetation	250x250m	16-day	3,4	30m	16-day
MCD43B3	Albedo	1 x 1km	8-day	2,4,7	30m	16-day

Figure 3.1: Flow chart of the UCLA-ET SEBAL-based model and implementation.



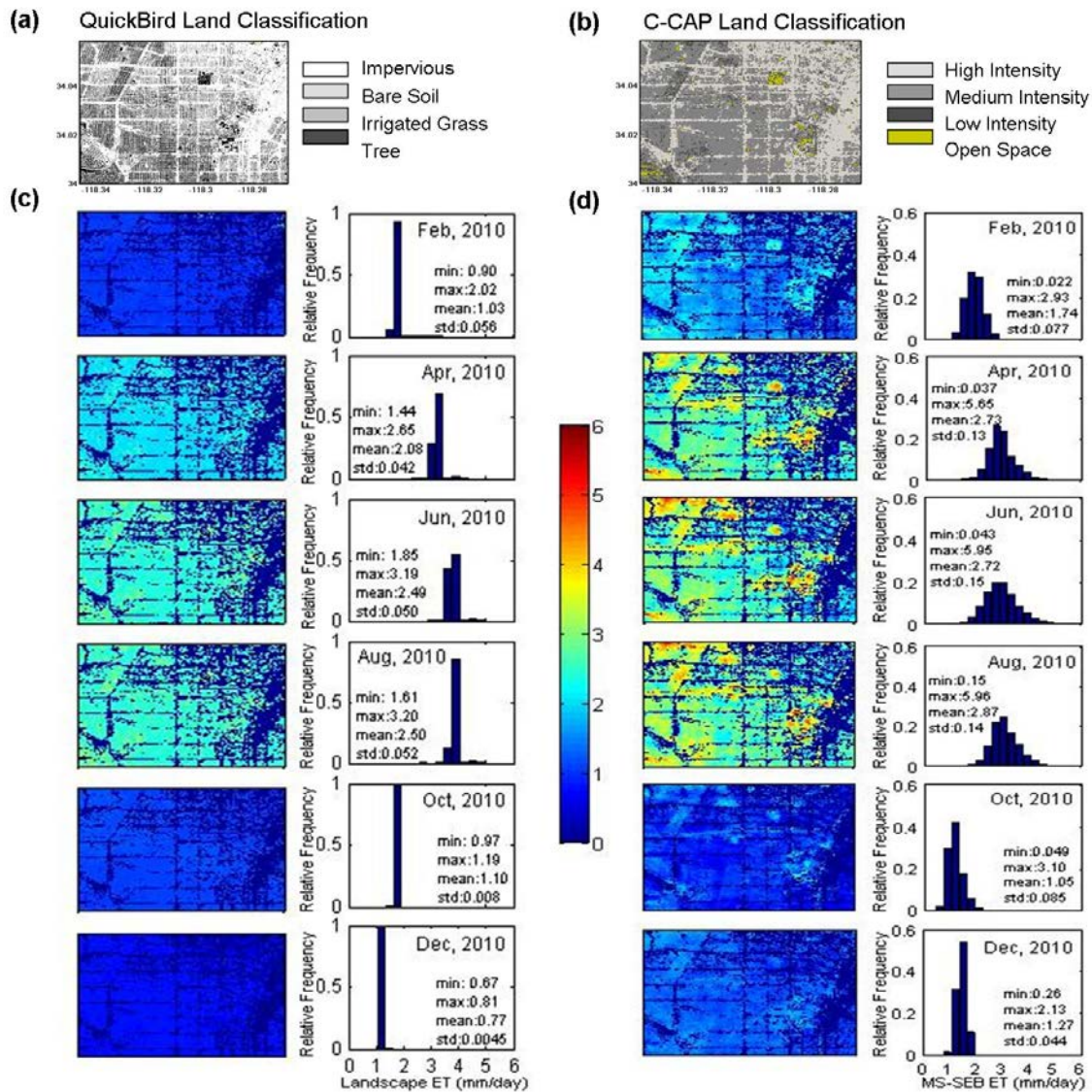
3.1.3 ET estimates for Los Angeles

In this project we evaluated the application of the UCLA-ET for highly urbanized Los Angeles. Previous applications of the model focused on natural ecosystems; for this project we selected a small urban domain (West of Los Angeles Downtown) that included different levels of development urban (open-land(1 percent), low intensity(7 percent), medium intensity(55 percent) and high intensity (36 percent)) for model evaluation (see Figure 3.2(b)). Each level contains different percentage of landscape (<20 percent (High intensity), 20 percent-49 percent (Medium intensity), 50 percent-79 percent (Low intensity), >80 percent (Open land)). In general, urban landscapes dominantly consist of turf grass, trees, and shrubs (Johnson and Belitz, 2012).

Spatial maps of monthly UCLA-ET and Landscape ET (PET adjusted with a landscape coefficient) during selected months in 2011 are presented in Figure 3.2(c) and (d) along with their relative frequency distribution. Spatially, the most significant feature of these results is that MS-SEB ET shows more variability throughout the study domain than Landscape ET. The landscape model using landscape coefficients (K_L) of 0.6 (Turf grass) and 0.65 (Tree) during warm season is likely too simple without considering vegetation density and species, water stress conditions, management practices, etc. For better spatial estimation, a more sophisticated

landscape model considering all these factors are required, if sufficient information is available (Eching and Snyder, 2005). However, this simple model provides a reference to evaluate whether our ET model is in a reasonable range.

Figure 3.2: Land cover imagery from (a) QuickBird satellite (b) NOAA's Coastal Change Analysis Program (C-CAP) over the west area near Downtown Los Angeles. The spatial distributions for monthly ET average (mm/day) and relative frequency distributions (bin size: 0.3mm/day) from (c) the Landscape Model and (d) the MS-SEB Model for selected months. Also minimum (min), maximum (max), mean and standard deviation (std) are also given.



The monthly comparison of irrigated ET values from UCLA-ET, Landscape ET and reference potential ET are presented in Figure 3.3. We found that the UCLA-ET model tends to

consistently overestimate ET as much as 1 mm/day (January through March on 2011) compared to the Landscape ET. While Landscape ET is about 44 percent of reference ET consistently throughout the year, the UCLA-ET is about 50 percent of reference ET during the summer season (May-July) and 70 percent during winter (November-January). This finding is similar to previous studies (Mayer et al., 1999) indicating that urban vegetation is about 60-80 percent of potential rate of ET. Even though a limited spatial comparison is shown in this study due to the lack of ground based data in our study domain, it is encouraging that the UCLA-ET model is generally showing higher spatial variability and much of the detailed spatial information while keeping the general spatial patterns and range in magnitude.

We examined the UCLA-ET model estimates for different land cover types over Los Angeles County. Five land cover types were selected including forest (deciduous forest, evergreen forest, and mixed forest), grass land, shrub lands, water bodies (lakes, aqueducts, etc.) and urban areas (open land to high intensity) (Figure 3.3). In general, the seasonal ET trends for all tested land covers are similar throughout the two years. ET starts to increase rapidly in April, reaches a peak in July, and then declines to the lowest levels in January. The results also show that water bodies have the largest average ET over the whole year, followed by forest. The lowest ET occurs in the developed areas.

The monthly ET for various urban development types are shown in Figure 3.4. As expected, the open land areas which contain the highest percentage of vegetation have the highest ET values throughout the study years. The lower the urban development level, the higher the annual ET values. We also note that the greatest variability in ET occurs in the urban development areas from April and September (from early spring to summer), whereas this difference is negligible in fall and winter seasons. Annual ET from open space is almost double the ET from the high intensity development space, while ET from medium and low intensity show smaller differences (Figure 3.4).

We also present UCLA-ET model results for the entire Los Angeles domain (Figure 3.5) for three select study days 2/ 11 (winter), 6/ 14 (late spring) and 9/ 7 (summer) during 2009. The distribution and patterns of ET are heavily affected by vegetation distribution and elevation variability. The spatial average of ET for the highlighted days, 2/ 11, 6/ 14 and 9/ 7, across the entire study domain are found to be 3.41, 4.35, and 5.53 mm/ day, respectively. The Santa Monica Mountains (upper left corner of domain) show relatively higher ET than most of the urban cover for all three images. We also note patches of elevated ET flux throughout regions of the city, especially parks and landscapes that are well-watered in the summer season (9/ 7 image).

Figure 3.3: Timeseries of monthly precipitation (mm/month) (top) and monthly CIMIS reference ET (CIMIS ETo- mm/month) (bottom) from the Glendale site. The monthly MS-SEB derived ET (mm/month) by land use/land cover types (i.e., Developed Area, Grass, Forest, Shrubland and Wetland) in the entire Los Angeles county.

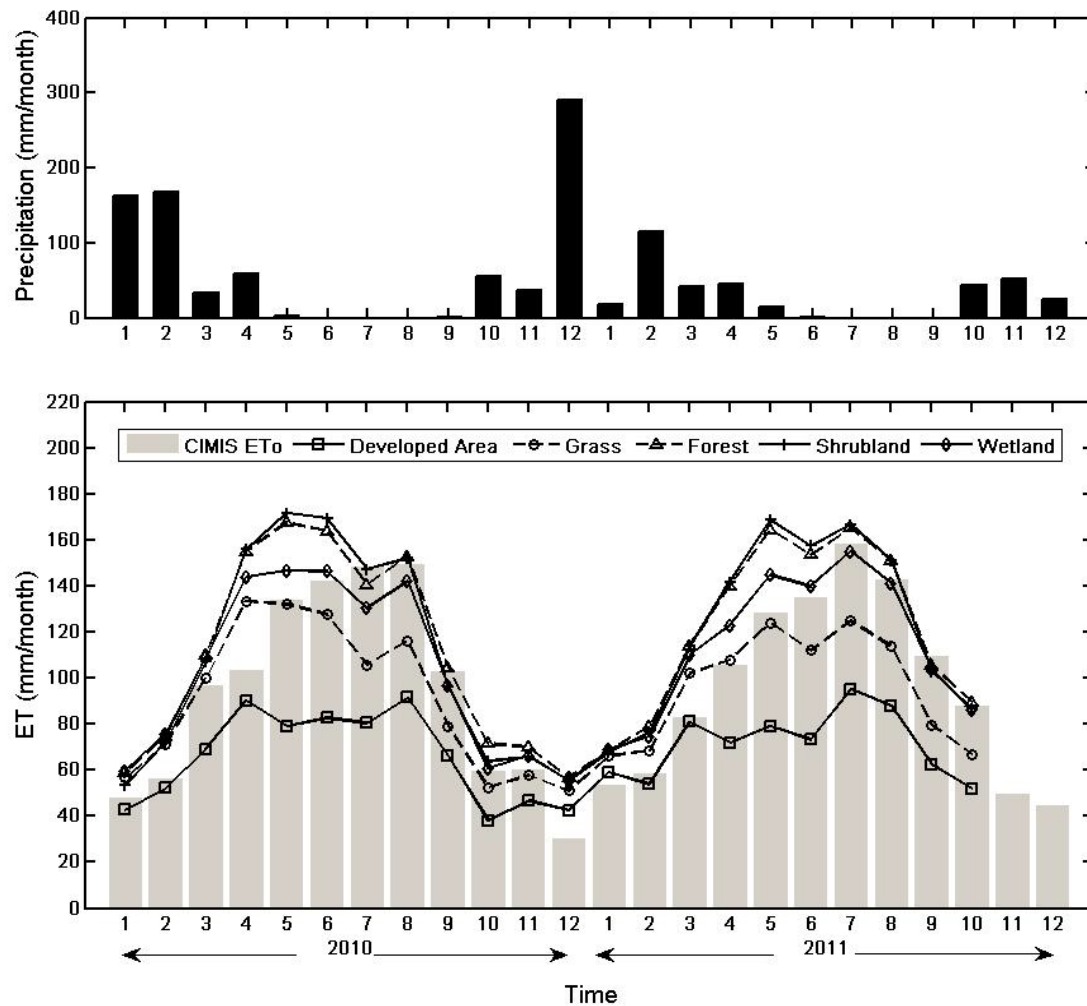
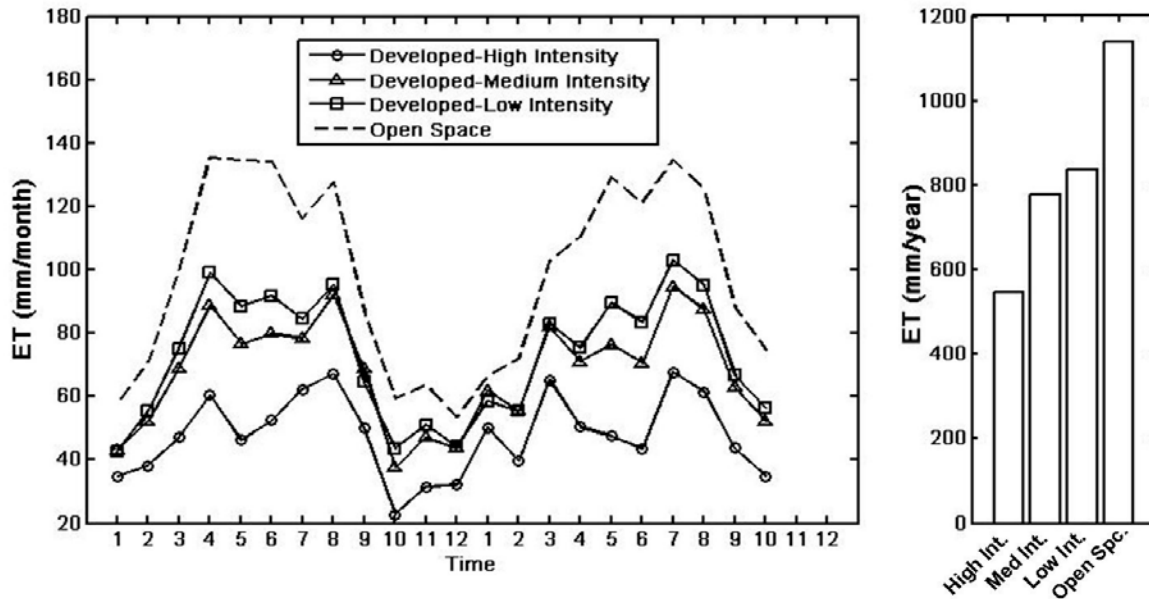


Figure 3.4: (Left) Monthly ET (mm/month) by development intensity (i.e., High, Medium and Low intensity and Open space) and (Right) Annual ET (mm/year) by different developed intensity in entire Los Angeles county.



3.1.4 Landscaping scenarios

To evaluate the sensitivity of urban ET to large scale landscape modifications, we performed a sensitivity analysis using a range of vegetation density scenarios. We selected three sub-areas from the larger domain to represent important microclimates and socio-demographics within the Los Angeles area, including the San Fernando Valley, Santa Monica and Hancock Park (Figure 3.6). We developed several scenarios of alternative vegetation cover, including decreasing cover or greenness (represented by NDVI) by 25 percent (-25) and 50 percent (-50), and also increasing vegetation cover by 150 percent (+150), respectively. ET is quite variable among the three selected regions, even though the vegetation index (NDVI) for each region is generally similar (0.21 to 0.25). Our baseline simulations show ET values of 2.5 mm/ day and 5.1 mm/ day for the San Fernando Valley and Santa Monica, respectively. Hancock Park has ET values more similar to the San Fernando Valley, with a mean ET of 2.95 mm/ day. There is also more variability in the ET values in the Santa Monica domain, with some pixels showing ET values up to 9.1 mm/ day. Peak values in Hancock Park and the San Fernando Valley are 6.6 mm/ day and 6.7 mm/ day, respectively. Our previous work in the region has shown that water consumption, and ultimately outdoor application, is highly influenced by the income of specific neighborhoods/ regions, with higher outdoor water consumption and resulting ET in higher income neighborhoods (Mini et al. In review). We note that the variability in the current ET simulations reflects a strong influence of socio-demographic variability across the region and less of an influence of climate on ET.

Figure 3.5: Los Angeles study domain with the UCLA SEBAL-based ET for study days 2/11 (winter), 6/14 (late spring) and 9/7(summer) in 2009.

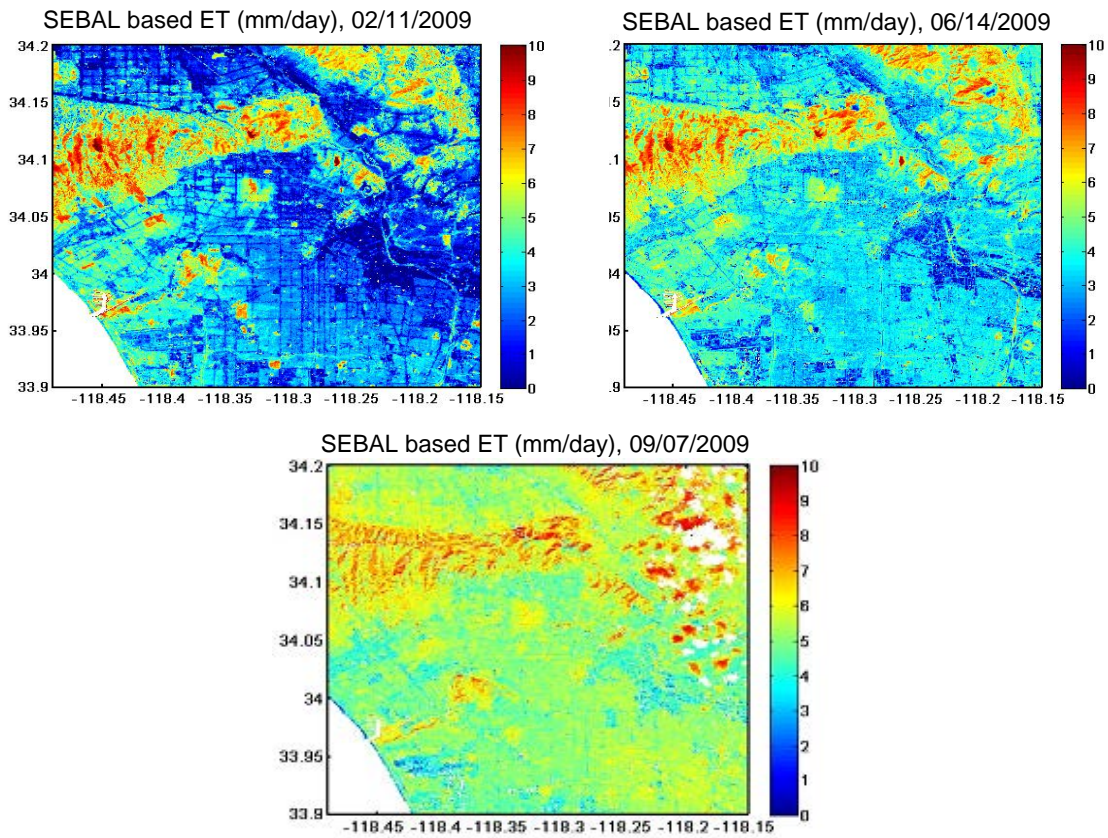
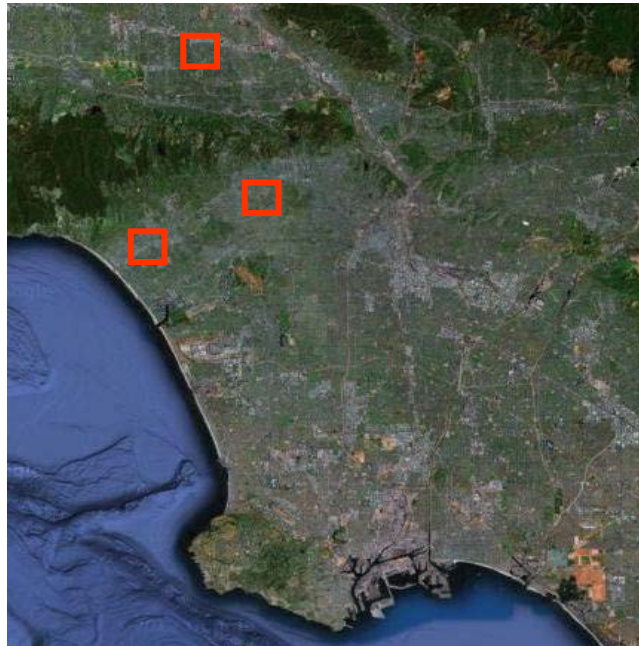


Figure 3.6: Los Angeles study domain with select areas (Santa Monica, Hancock Park and the San Fernando Valley) used in sensitivity analysis of vegetation cover.



Results from the vegetation change scenario for each region indicate that ET is consistently influenced by changes in the amount of plant biomass (Figure 3.7). A decrease of 50 percent in biomass in our ET model, theoretically representing a 50 percent decrease in the density of landscape vegetation, in the three region results in reductions in ET of 1.6, 4.4, and 2.3 mm/ day for the San Fernando Valley, Santa Monica and Hancock Park regions, respectively. Assuming simple averaging across each region, these reductions in landscape ET result in overall reductions in water consumption of 5.7, 4.4, 4.5 acre-feet (AF) for the chosen study day across each region. Extrapolating these results to an annual value (June ET fluxes are in the mid-range of the yearly values), results in annual water savings of 2081, 1606, 1642 AF/ year for each of the study regions (they are each 25km² in area). The City of Los Angeles is approximately 1300km² in area. If we do a simple extrapolation to a city-wide model of a 50 percent reduction in biomass, and using the lowest annual water savings seen in one of the study areas (1606 AF/ year), the city may potentially reduce landscape water consumption by 83,512 AF/ year. This equates to just over 10 percent of the city's annual water use of around 650,000 AF/ year (LADWP, 2011). We note that this is a relatively simple extrapolation from the select study domains to a city-wide estimate and a more comprehensive sensitivity analysis is currently underway to support these initial estimates.

Figure 3.7: Example of spatial patterns resulting from vegetation sensitivity analysis in the San Fernando Valley domain.

San Fernando Valley

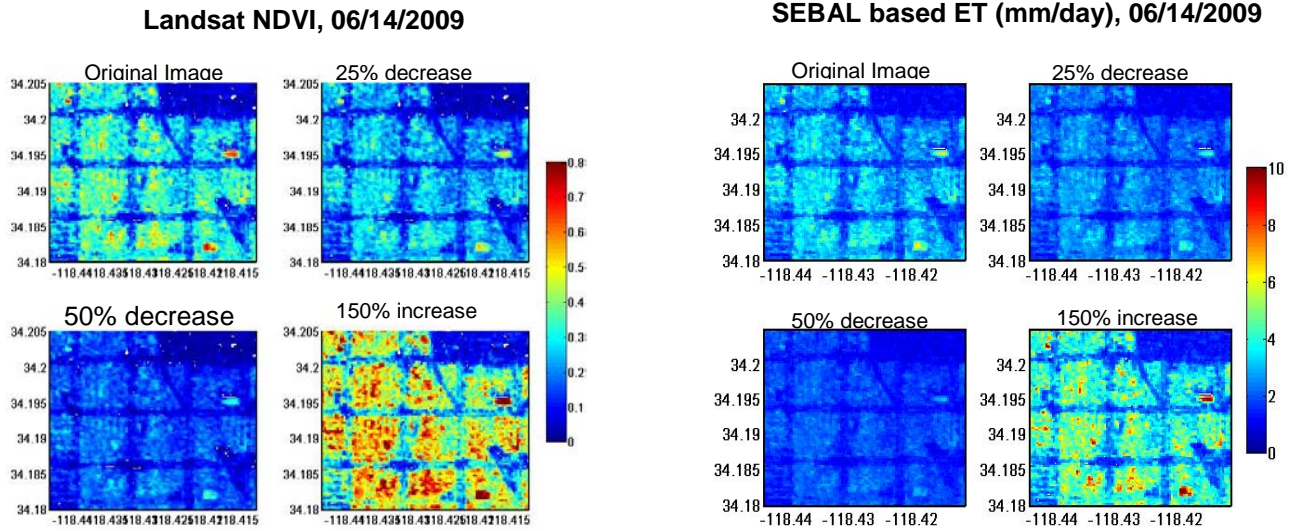


Table 3.2: Results from sensitivity analysis for three select locations. Table includes NDVI and ET results for a select study day in June, 2009.

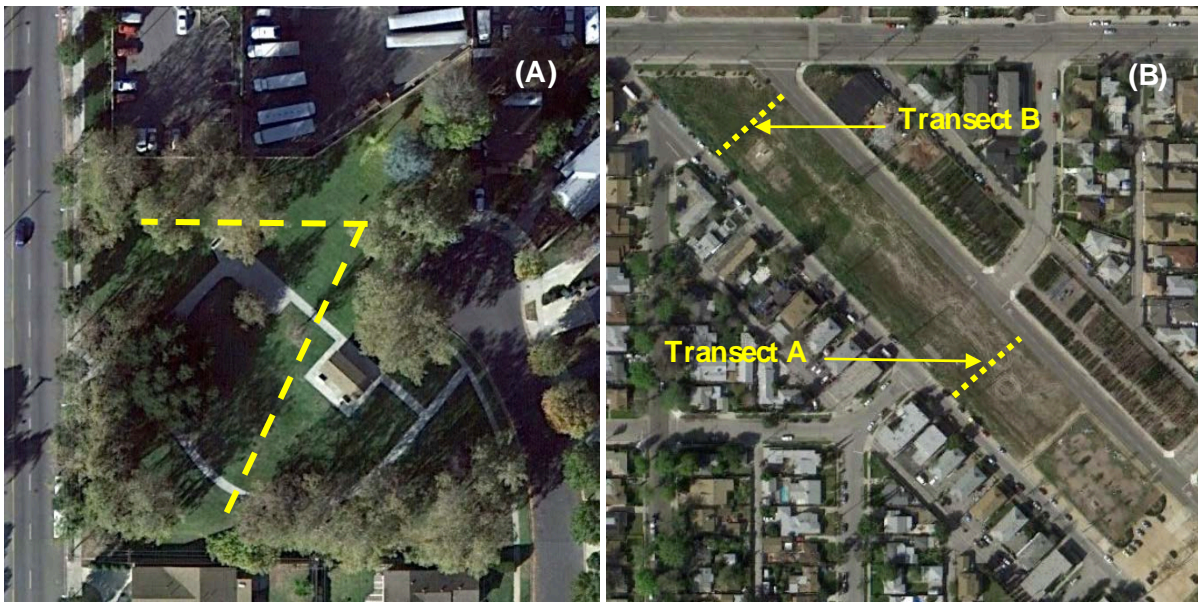
		NDVI				ET				
Location	Change	Mean	Std	Min	Max	Mean	Std	Min	Max	ET (AF/day)
SF Valley	Original	0.25	0.020	0.000	0.75	2.51	0.14	0.74	6.66	16.82
	-25%	0.18	0.015	0.000	0.56	2.08	0.10	0.74	4.63	13.90
	-50%	0.12	0.010	0.000	0.37	1.66	0.06	0.72	3.25	11.12
	+150%	0.37	0.030	0.000	1.13	3.48	0.28	0.74	13.24	23.32
Santa Monica	Original	0.21	0.025	0.003	0.77	5.07	0.17	2.66	9.06	33.92
	-25%	0.15	0.019	0.002	0.58	4.74	0.12	2.66	7.48	31.68
	-50%	0.10	0.013	0.002	0.38	4.41	0.07	2.65	6.18	29.51
	+150%	0.32	0.038	0.005	1.16	5.79	0.36	2.68	13.69	38.76
Hancock Park	Original	0.21	0.017	0.000	0.71	2.95	0.13	1.46	6.57	19.72
	-25%	0.16	0.013	0.000	0.53	2.60	0.08	1.46	4.92	17.39
	-50%	0.10	0.008	0.000	0.35	2.26	0.05	1.46	3.75	15.13
	+150%	0.32	0.026	0.000	1.06	3.70	0.25	1.46	11.62	24.74

3.2 ET measurements in the model domain

3.2.1 Study Areas

Two study sites were selected to measure grass ET for comparison to the UCLA-ET remote sensing model. The two sites are located at Jesse Owens Mini Park in Reseda, CA and Whitnall Highway Park in North Hollywood, CA (Figure 3.4). Jesse Owens Mini Park, hereafter referred to as Jesse Owens, experienced average temperatures of 16.7 °C over the sampled year (November 2010 to October 2011) and received a cumulative total of 556 mm of precipitation during this time. The precipitation data was provided by the National Climatic Data Center (NCDC) weather station located 2.9 km northeast at the Van Nuys Airport. Precipitation values for the study period at Jesse Owens are much higher than the historical thirty-year average (1980-2010) while the average temperature about 1°C below the average (Table 3.3). In addition, Jesse Owens receives more rainfall than Whitnall Highway and has a similar average temperature over the study period.

Figure 3.8: Transect layouts and plan view of the sampled sites. A) Jesse Owens Mini Park in Reseda, CA. B) Whitnall Highway in North Hollywood, CA



Jesse Owens is well irrigated and is maintained by the City of Los Angeles. It is uniformly covered with Bermuda turfgrass (*Cynodon* spp.) with a total area of approximately 6475 m², including approximately 680 m² of concrete pathways or structures throughout the park. Bermuda grass has medium drought tolerance and is categorized as having medium to high moisture use (United States Department of Agriculture, 2011). An array of trees encompasses the park, mainly composed of California Sycamore (*Platanus racemosa*), with an assortment of other species, including Live Oak (*Quercus agrifolia*) and Ginkgo (*Ginkgo biloba*).

Nine miles east of Jesse Owens, Whitnall Highway is an unmanaged, non-irrigated strip of land located in a residential area, situated between two parallel streets. The site is dominated by exotic annual herbaceous species including hare barley (*Hordeum murinum*), wild oat (*Avena fatua*), long-beaked storksbill (*Erodium botrys*) and doveweed (*Croton setigerus*). The site experiences a similar climate to Jesse Owens, with a yearly average temperature of 17.2 °C and 441.45 mm of observed precipitation during the sampling period. Whitnall Highway receives more rain historically, but received less during the study period (Table 3.3). The NCDC weather station providing precipitation data is located 2.7 km north at the Burbank Airport. Whitnall Highway covers approximately 11980 m² in area with a small, unvegetated area measuring about 96 m² in the middle of the park. Prior to the May set of measurements, the site appeared to be mowed and cut, removing nearly all the vegetation. This left the park covered in the remains of the cut vegetation and only approximately 10-15 percent of vegetation cover based on a visual estimation. There was some regrowth after this, until the site was mowed again prior to the September set of measurements, leaving approximately 5 percent vegetation cover throughout the park. The vegetation showed renewed signs of regrowth in October.

Table 3.3: Past and present meteorological data from National Climatic Data Center gauges. The sampled period (Nov 2010-Oct 2011) is compared with the previous five water years. Thirty-year averaged historical data (1980-2010) is from the Western Regional Climate Center.

Water Year	Van Nuys (Jesse Owens)			Burbank (Whitnall Highway)		
	T [°C]	RH [%]	Ppt [mm]	T [°C]	RH [%]	Ppt [mm]
Study Period	16.7	0.60	556.00	17.2	0.60	441.45
2010	17.4	0.56	441.45	16.8	0.59	375.16
2009	18.7	0.52	275.08	18.0	0.57	253.49
2008	18.3	0.53	293.12	17.6	0.53	246.63
2007	18.2	0.52	113.03	17.4	0.53	63.75
2006	18.2	0.57	384.05	17.7	0.58	346.46
Historical (1980-2010)	18.0	--	359.16	18.3	--	441.20

3.2.2 Measurements

3.2.2.1 Frequency of Measurements

Evapotranspiration and meteorological variables at each site were measured three times a week during one week per month over the span of approximately one year. Measurements at Jesse Owens were taken from November 2010 to October 2011 while measurements for Whitnall Highway were recorded from January 2011 to October 2011. During two of the three monthly sampling dates, ET and meteorology was recorded from 10 am to 2 pm while data for the third sampling date was recorded from 10 am to 4 pm. Measurement times were chosen to capture diurnal patterns including maximum daily ET. Within each sampling date, measurements were taken on the hour, every hour until the end of the sampling period. Due to weather and scheduling conflicts, occasionally only two measurement days per month could be obtained for the sites.

3.2.2.2 Transects for ET Measurements

At Jesse Owens, a transect was marked from the southwest corner to the northwest corner of the park spanning approximately 53 meters, along which ET was measured. There were five sampling points along this transect, with additional sampling points at the northwest and southwest corners of the park. The transect was designed to incorporate both sunny and shaded areas of the site (Figure 1). Each point along the transect was separated by approximately 13 m. At least one point was in the shade during each measurement period. Due to the size and vegetation variability at Whitnall Highway, a different approach was used to establish the transect. A set of measurements was made using a zigzag pattern across the park to encompass all parts of the site. These initial measurements showed that the northwestern portion of the park had higher ET as well as greater biomass (estimated by visual inspection) than the southeastern portion. As a result, two separate transects were used to represent the park, one spanning the width of the southeast section and one spanning the width of the northeast section (Figure 1). The transects were chosen to span the width of the park to account for differences in vegetation density in the eastern and western sides of the park.

3.2.2.3 Data Processing

ET was measured using the chamber method described in Chapter 2. To extrapolate instantaneous measurements to the daily scale, we used the Clausius-Clapyeron equation, with the saturated vapor pressure was calculated as:

$$e_s = 611 \exp\left(\frac{17.3T}{T + 237.3}\right) \quad (3.9)$$

Where e_s is the saturated vapor pressure (Pa) and T is the measured temperature inside the chamber ($^{\circ}\text{C}$). To convert the saturated vapor pressure to partial vapor pressure, the relationship between saturated partial vapor pressure and relative humidity was employed:

$$e = \frac{RH \cdot e_s}{100} \quad (3.10)$$

Where e is the partial vapor pressure (Pa) and RH is the measured relative humidity inside the chamber (%). Next, the ideal gas law can be applied to calculate the mass flux of water for each measurement:

$$\rho_v = \left(\frac{e}{R_v T}\right) \quad (3.11)$$

Where ρ_v is vapor density (kg water/ m^3), R_v is the water vapor gas constant (461.87 J kg K) and T is the temperature in Kelvin.

Once the raw data had been converted to a vapor density, the data was plotted against time. Each hourly measurement was evaluated individually. Within the hour, seven (Jesse Owens) or ten (Whitnall Highway) measurements were made. Each measurement was inspected to find the steepest slope of the relationship between vapor density and time. Due to some inconsistent slopes, particularly at Whitnall Highway, the steepest slope was generally found over five consecutive data points, accounting for 10 seconds inside the chamber. These points were used to find a slope representing the constant slope section as used by McLeod et al (2004). This slope is then used to estimate ET (mm/ h) in the equation provided by Stannard (1988):

$$ET = 0.0036 \frac{M \cdot V \cdot C}{A} \quad (3.12)$$

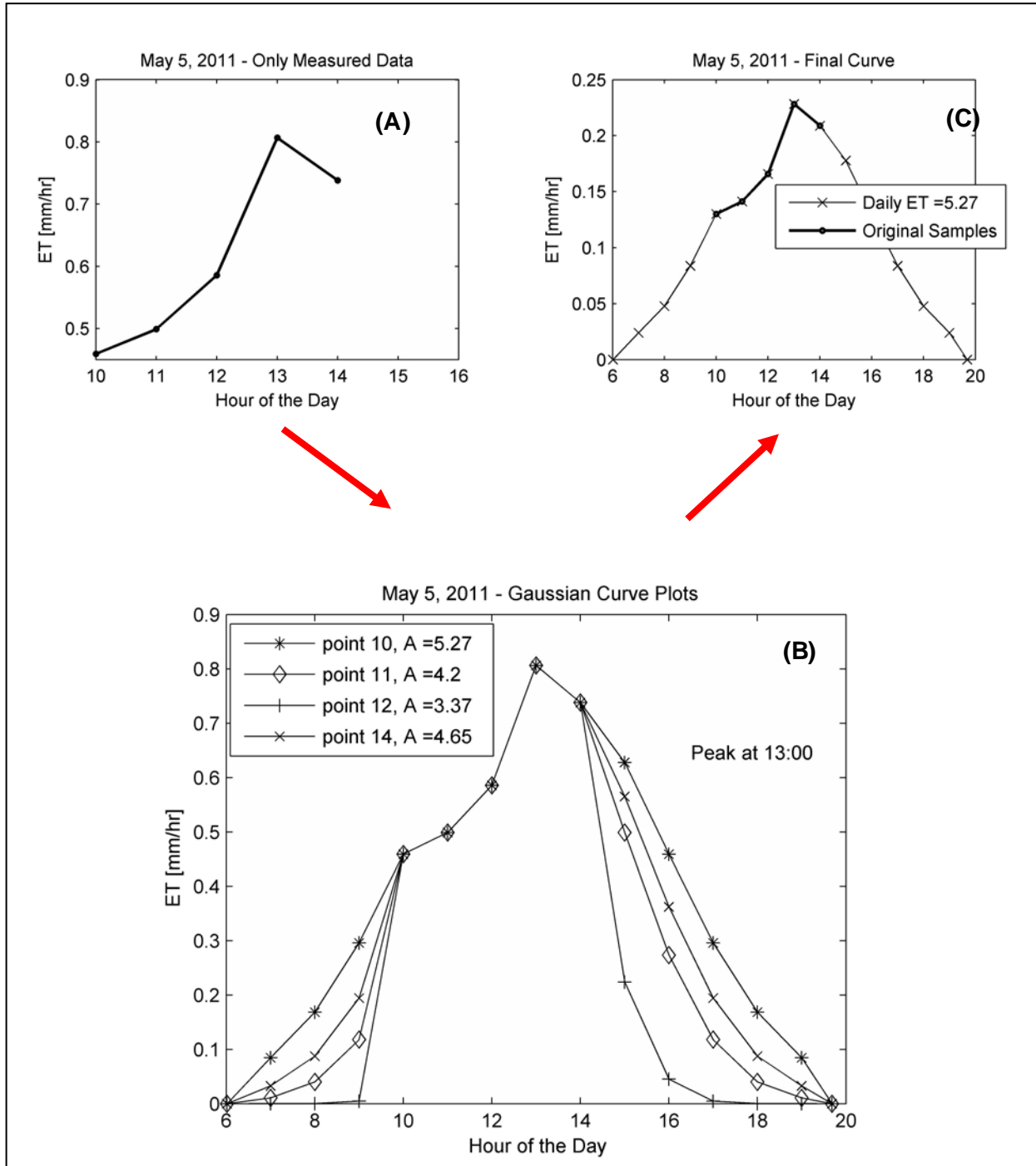
Where M is the steepest portion of the slope of the vapor density plot (mg/ m^3), V is the volume of the chamber (m^3), A is the area of the ground covered by the chamber (m^2), C is a calibration factor accounting for any vapor absorption by chamber walls, and 0.0036 is a conversation factor to convert from mg/ m^3 to mm/ hour . In this study, the calibration factor, C , was set to 4.26 as developed by Litvak et al. (In review). This calibration factor was obtained by comparing chamber ET values to weighing lysimeter values (prior work by UC-Irvine). The instantaneous ET values at each point along the transect were averaged to find the hourly ET for the transect. Depending on the measurement day, the estimated values only accounted for five or seven hours of the day. To establish daily ET, a Gaussian function was employed:

$$y = a * \exp\left(\frac{-(t - t_0)^2}{2b^2}\right) \quad (3.13)$$

$$b^2 = \frac{-(t - t_0)^2}{2 \ln\left(\frac{y}{a}\right)} \quad (3.14)$$

Where y is the ET value at a given time (mm/ h), a is the maximum daily ET (mm/ h), t_0 is the time of peak ET, t is the time being evaluated and b is a factor controlling the width of the curve. The limits of the curve were set using sunrise and sunset data from the US Naval Observatory. At these times, ET was set to zero, assuming that there is minimal ET before sunrise and after sunset. Equation 6 was set equal to b and used the measured ET values for y and t to solve for b . Since multiple values for y and t could be used to solve for b , an ensemble of curves was plotted using all measured ET values (Figure 3.5). Typically, the lesser of the two middle curves were used, unless a different curve better followed the smooth shape of a typical, diurnal pattern. The curve of the longer measurement day (10:00 am to 4:00 pm) was used to evaluate the expected shape of the diurnal pattern of ET for that week. The area underneath the curve represents cumulative ET in mm/ day.

Figure 3.9: Example of using Gaussian function to complete the curve from Jesse Owens Mini Park on May 5, 2011. A) A plot of the calculated hourly ET from measured data. B) Resultant ensemble curves using a respective hourly ET point to solve the Gaussian equation. The areas under the curves are listed in millimeters in the legend. C) The finalized ET curve after choosing the most appropriate point and curve from the ensembles.



3.2.2.4 Modeling Daily ET

There were limited measurements per month at each site over the course of the study period. In order to extrapolate more temporal ET data from these measurements, a multi linear regression function in MATLAB was used to create an equation to find daily ET rates based on measured ET data. The regression utilized solar radiation and VPD, and estimated coefficients corresponding to these variables to best predict ET rates found in the field:

$$ET = A \cdot (SolarRadiation) + B \cdot (VPD) \quad (3.15)$$

Unfortunately, daily measurements of solar radiation and VPD values were not available at each respective site. As a result, California Irrigation Management Information Systems (CIMIS) station values were used in conjunction with the measured ET values to obtain coefficients A and B for the multi linear regression model. The coefficients account for the differences between the respective CIMIS and measured solar radiation and VPD data. The model utilizing the coefficients based on CIMIS data was then used to find daily ET values, relying only on solar radiation and VPD.

In order to more closely model the trends of ET and the relationship with solar radiation and VPD, the regression model was broken down seasonally and into wet and dry seasons. The wet season for this study is defined as November to April and the dry season covers May to October. The seasonal breakdown is as follows: NDJF (November 2010 to January 2011 – winter), MAM (March to May – spring), JJA (June to August – summer) and SO (September to October – fall). Different coefficients were established for each season. A composite of all or both seasons was created to establish an estimate of daily ET over an entire year for both methods. It is hypothesized that the seasonal model will perform best, assuming the smaller sample size will establish coefficients representing the strongest relationships between ET and the meteorological variables.

3.2.2.5 Statistical Analysis

Two methods were used to test the significance of the results from the study. A Student's t-test was used to validate the differences between all measured ET values (33 for Jesse Owens, 28 for Whitnall Highway) observed at the two parks. A heteroscedastic test was employed with a 95 percent confidence level ($\alpha=0.05$), testing a null hypothesis that the mean of measured ET at Jesse Owens is the same as the mean of measured ET at Whitnall Highway. ET values were separated seasonally as discussed in the previous section and were evaluated for statistical differences between the study sites. A heteroscedastic Student's t-test with $\alpha=0.05$ was used to compare seasonal ET values at both study sites, testing for a hypothesized mean difference of 0. A one-way Analysis of Variance (ANOVA) was performed to evaluate the significance of different relationships between ET and meteorological data as well as the daily multi regression model ET and daily CIMIS ET. The F-test was used to provide statistical significance at a 95 percent confidence level. These evaluations will enable us to understand and identify the significant drivers of ET as well as significant relationships at each site. To evaluate the performance of the developed multi linear regression model, four metrics were used to compare modeled ET to actual measured ET: daily root mean squared error (DRMS), Nash-Sutcliffe efficiency (NSE), percent bias and Pearson's correlation coefficient.

3.2.3 Results and Discussion

3.2.3.1 Site ET Comparison

As expected, the parks illustrated very different patterns of ET over the study period (Table 3.4) Jesse Owens showed more ET than Whitnall Highway, as hypothesized ($p < 0.05$). In general, the pattern of ET was different between parks, with some peaks in ET for one park corresponding with low ET for the other park. In both cases, ET was negatively correlated with relative humidity (figure not shown). Some correlation is expected, as relative humidity is related to the VPD, a typical driver of ET. Though Whitnall Highway showed a higher correlation with relative humidity, only ET at Jesse Owens showed a significant relationship and good correlation ($R^2 = 0.68$) with VPD, presumably due to the summer dormancy of unirrigated grass at Whitnall.

Table 3.4: ET measurements recorded at the two parks From November 2010 to October 2011. Typically, three measurements were taken each month with a few exceptions. Measurements for Whitnall Highway began in January 2011. All values are in mm/day.

	Nov	Dec	Jan	Feb	Mar	Apr	May	Jun	Jul	Aug	Sep	Oct
Jesse Owens	4.18	1.54	0.92	2.50	1.95	3.88	8.09	5.70	5.03	9.99	4.76	4.61
	NaN	0.69	1.42	2.24	4.90	2.42	6.01	5.78	4.58	7.73	4.45	1.30
	NaN	0.10	1.82	2.21	2.37	1.64	3.35	4.40	NaN	5.92	5.16	2.55
Whitnall Highway			2.32	1.38	2.43	0.68	0.86	1.40	0.67	1.45	0.80	1.13
			2.53	1.59	0.77	2.47	1.20	0.77	0.97	1.41	0.87	1.04
			2.72	0.44	NaN	NaN	0.89	0.69	0.64	1.00	1.09	0.72

In general, ET at Jesse Owens parallels the behavior of potential evapotranspiration (PET). PET is considered to be the maximum possible ET and is based on the assumption that the area of interest has an unlimited or sufficient water source and that stomatal control of transpiration is not important (Dingman, 2008). PET is largely driven by climate, such as radiation, temperature and VPD (Thornthwaite, 1948). The correlation with these factors indicates that Jesse Owens has an ample amount of available water and that the grasses showed limited stomatal closure at high VPD. Since Whitnall Highway is non-irrigated, the main water source for the park comes from precipitation. Precipitation seems relatively unrelated to ET at Jesse Owens, as the highest values come months after the last rainfall event. The largest quantities of precipitation during the study period occurred at the end of December and at the end of March, yet ET was relatively low at this time. The highest ET occurred during a consistent period without precipitation. Whitnall Highway, in contrast, showed the highest ET during or just following precipitation in January, March and April.

3.2.3.2 Seasonal Comparison

Table 3.5 shows the seasonal averages of ET at the two study sites. Whitnall Highway and Jesse Owens both showed average ET rates of 1.8 mm/ day for the winter season. During the summer, Jesse Owens had the highest ET values, averaging 6.1 mm/ day and a peak value in August of 10.0 mm/ day. Meanwhile, Whitnall Highway only showed an average of 1.0 mm/ day of ET in summer. These results show the magnitude of the change in ET resulting from urban irrigation relative to unirrigated land cover in Los Angeles.

Table 3.5: Seasonal Averages of ET for both parks.

	Jesse Owens	Whitnall Highway
Winter	1.76	1.83
Spring	3.85	1.33
Summer	6.14	1.00
Fall	3.81	0.94
Yearly	3.89	1.28

It is interesting to note that although winter is the season of peak ET for Whitnall Highway and the season of lowest ET for Jesse Owens, the two parks show very similar ET during this time. Therefore, during the winter wet season, irrigated and unirrigated grass ET appears to be similar in Los Angeles.

3.2.3.3 Comparison with Previous Studies

The observed ET values are comparable to published ET values from an eddy correlation study in the Los Angeles area (Grimmond and Oke 1999) (Table 3.5) and reference ET calculations made by CIMIS. The sites studied by Grimmond and Oke (1999) were only 25 percent grass cover, whereas the sites in this study are at least 90 percent grass or vegetation. If the reported daily ET values from Grimmond and Oke are scaled up from 25 percent cover to 90 percent cover, ET is similar between San Gabriel, Arcadia and Jesse Owens (Table 3.5), which are all irrigated areas in southern California. Jesse Owens yields an average of 7.0 mm/ day during the month of July, which falls in the range of the scaled values of 5.0 mm/ day and 7.6 mm/ day for San Gabriel and Arcadia, respectively. Whitnall Highway shows much lower ET in July at 0.7 mm/ day due to the lack of irrigation. Previous measurements of non-irrigated grass in the Los Angeles area are not available.

Table 3.6: Published urban ET values from Grimmond and Oke (1999) compared to values in the current study. Published values are scaled to 90% vegetation cover for comparison to Jesse Owens and Whitnall Highway ET values.

Site	Published ET [mm/ day]	Scaled ET [mm/ day]	Irrigation
San Gabriel, July 1994	1.4	5.0	Extensive
Arcadia, July 1994	1.9	7.6	Extensive
Arcadia, July 1993	2.0	7.5	Extensive
Jesse Owens, July 2011	7.0	7.0	Extensive
Whitnall Hwy, July 2011	0.83	0.83	None/ Natural

We also compare our results to the developed models published in the Los Angeles Department of Water and Power Urban Water Management Plan from 2010, hereafter referred to as the Plan. We assume that there was little to no change in the water usage between 2010 and 2011, allowing the results to be compared. The Plan specifically focuses on irrigated areas, so only the irrigated model from Jesse Owens is relevant. The Plan uses reference ET provided by the Model Efficient Landscape Ordinance for the City of Los Angeles (Repp, 2012). It is derived from a combination of sources including CIMIS, the Reference ET Zones Map from the UC department of Land, Air and Water Resources and California Department of Water Resources and Reference ET for California from the University of California Department of Agriculture and Natural Resources (City of Los Angeles, 2012). In general, the CIMIS station data is used to estimate reference ET values for the Plan. To calculate water necessary for irrigation (LADWP, 2011):

$$LW = 0.62(ET_o - Eppt) \cdot A \cdot ETAF \quad (3.14)$$

Where *LW* is estimated total supplemental water needed for landscape irrigation (gal/ yr), *ET_o* is reference evapotranspiration (in/ yr), *Eppt* is effective precipitation (25 percent of monthly precipitation, in/ yr), *A* is total greenscape area (irrigated grass and tree canopy cover, ft²) and *ETAF* is an ET adjustment factor. The 0.62 coefficient is a conversion factor to gallons. The *ETAF* is based on a combination of plant factor and irrigation efficiency, and is set to 0.8 for Los Angeles (LADWP, 2011). The greenscape area is calculated to be approximately 83,699 acres. This includes 31,206 acres of irrigated grass and 52,493 acres of tree canopy cover, including shrubs, representing 12 percent and 21 percent of the area of Los Angeles, respectively (McPherson et. al, 2007). Using Equation 3.14, the Plan estimates 249,000 AF of water is used annually for outdoor landscaping (LADWP, 2011). The regression model for Jesse Owens estimates 1181 mm of annual ET (Table 3.6).

Applying this value to the area of irrigated grass in Los Angeles as determined by McPherson et al. (2007), the Jesse Owens seasonal model estimates a total of approximately 120,000 AF of ET for the study period. This represents 45 percent of all water used for irrigation, while representing just over 36 percent of the total greenscape in the city. In 2010, the total water demand for the City of Los Angeles averaged 647,000 AF (LADWP, 2011). This suggests that ET

loss from irrigated turfgrass represents 18.5 percent or nearly one-sixth of the entire water demand for Los Angeles. Table 3.7 displays the modeled monthly ET values in comparison to CIMIS monthly ET values used by LADWP in Equation 13. As described in Chapter 2, CIMIS calculations data tends to overestimate ET, so we can assume that the 45 percent is an underestimation of the total amount necessary for irrigation. It is understood that scaling this model to such a large area comes with high uncertainty and many assumptions, so this analysis is intended to provide a first order approximation of actual annual water loss by ET from irrigated turfgrass in Los Angeles.

Table 3.7: Jesse Owens seasonal model and reference ET rates used by LADWP (Repp, 2012) in millimeters. Modeled ET values span from Nov 2010-Oct 2011. Reference ET is from Jan 2010-Dec 2010.

	Jan	Feb	Mar	Apr	May	Jun	Jul	Aug	Sep	Oct	Nov	Dec	Annual
Model	49.4	31.6	79.7	98.1	94.7	119.8	167.4	177.7	139.4	137.5	54.5	31.2	1181.3
LADWP	55.9	68.6	94.0	119.4	139.7	147.3	157.5	149.9	127.0	99.1	66.0	48.3	1272.5

3.3 Model-data comparisons

Finally, we compared output from the UCLA-ET Model with the ground-based studies at Jesse Owens and Whitnall Highway. In figure 3.10(a) and (d), we compare ET at each satellite overpassed time (11am to 12:30pm) against chamber ET at the same time by using the linear interpolation between 11am and 1pm hourly measurements. To examine the performance of the interpolation technique for EF during cloudy sky pixels, we have separated results into clear days (directly retrieved from SEBAL model) and all-sky condition days including both clear and cloudy days. The results during clear sky days showed a correlation (R) of 0.39 and RMSE of 0.14 (mm/ hr) for Jesse Owens and correlation (R) of 0.14 and RMSE of 0.11 (mm/ hr) for Whitnall Highway during all sky condition. For all sky days, while the correlation decreases to 0.29 and RMSE increases to 0.23 at Jesse Owens, the results significantly improved by increasing correlation from 0.14 to 0.80 and both RMSE and Bias are also decreased over Whitnall Highway site.

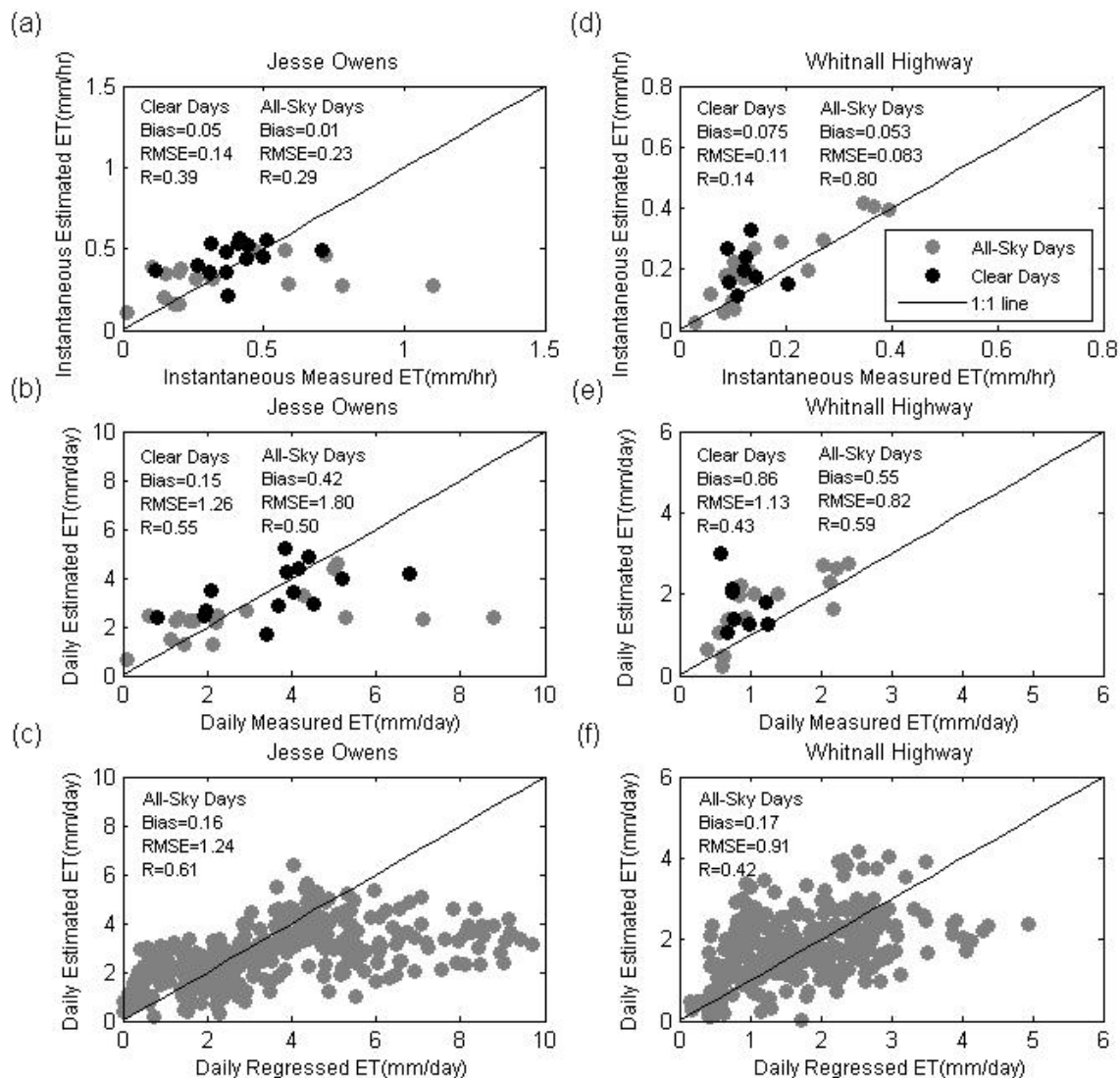
At the Jesse Owens site, discrepancies greater than 0.2 mm/ hr occurred when the chamber measured ET reached a peak during dry periods (i.e. DOY 68, 123 and 214 at Year 2011). This may be related to the extra soil moisture added by irrigation and higher energy forcing during those days. This result indicates that our temporal interpolated EF using neighboring days does not currently capture peak ET due to irrigation. However, at the non-irrigated Whitnall Highway site, the performance of the UCLA-ET model temporal interpolation scheme is able to reproduce ET well for all days without uncertainty associated with irrigation, although the results tend to be slightly overestimated.

Comparisons of daily average of ET are also shown In Figure 3.10(b) and (e). Although there are occasions when the algorithm has large biases, for example, a 2.5 mm/ day difference at DOY 193 in 2011, in which errors appear to be propagated from the uncertainty of sinusoidal model extrapolating instantaneous to daily average, it has a consistent overall performance for both

Jesse Owens and Whitnall Highway. The range of correlation is 0.43 and 0.59 and RMSE is between 0.82 and 1.80 mm/ day.

In addition to the chamber measurement data (32 and 28 for Jesse Owens and Whitnall Highway, respectively), the daily time-series of ET estimates were generated using multi linear regression model based on the measured data. The comparisons of daily average ET from the UCLA-ET model with the chamber regression daily ET are highlighted in Figure 3.10(c) and (f). On average, the correlation coefficient is 0.61, RMSE is 1.24 mm/ day and Bias 0.16 for Jesse Owens; while the correlation coefficient is 0.42, RMSE is 0.91 mm/ day and Bias 0.17 for Whitnall Highway. Considered relatively large errors of regression ET data at Whitnall Highway, the overall performance for both sites at daily basis is within an acceptable error range. The monthly comparison (not shown here) is further improved between the two approaches.

Figure 3.10: Scatter plots of MS-SEB ET against Chamber Measured ET at instantaneous satellite overpassed time (a and d), at daily average (b and e) and Scatter plot of MS-SEB ET against Chamber Regressed ET at daily basis (c and f) for Jesse Owens and Whitnall Highway, respectively. Also Bias, RMSE (Root Mean Square Error), and Pearson Correlation Coefficient (R) are also presented.



CHAPTER 4:

Conclusions and Recommendations

In this study we evaluated the potential for adaptation to California's declining water supplies through reductions in outdoor water use in the Los Angeles area. We studied the factors that influence urban evapotranspiration (ET) from the plot to the regional scale with direct measurements and modeling of ET. To date, *in situ* measurements of the water use of urban plants have been lacking, and computational methods that account for the high degree of spatial variability in urban ET have also been limited. This research presents methods of reducing these uncertainties and advances our understanding of the potential for reducing urban outdoor water use in southern California, a region where urban water availability and outdoor water consumption are increasingly of concern.

4.1 Options for reducing outdoor water consumption

Urban areas show a very high degree of spatial and temporal variability in ET due to the many modifications to the water cycle that result from urbanization. In Los Angeles, most urban vegetation is irrigated, although irrigation practices vary by land owner. Urban vegetation has also been highly modified in both the type and amount of vegetation now present in the Los Angeles Basin. Due to the mild climate, many species have been imported into Los Angeles from around the world; the Los Angeles urban forest shows a very high degree of biodiversity relative to the natural forests of southern California. Variability in water inputs by homeowners and land managers, diverse water and land management practices, novel assemblages of species, and high biodiversity make predictions of ET very complex. We conducted both observational studies and experiments to distinguish among the many factors that influence urban ET. These include:

- *Species composition* – urban vegetation in Los Angeles bears little resemblance to the native land cover, and may consist of various assemblages of trees from diverse regions, lawns, and diverse herbaceous and shrub groundcover. Transpiration rates and its response to environmental conditions varies greatly by species and plant functional types.
- *Spatial configuration of landscape types* – in addition to biodiversity, the precise location of vegetation types and their spatial relationship may greatly influence surface energy balance and the resulting rates of ET. For example, shade trees greatly reduce incident radiation below the canopy, and therefore may have a disproportionate effect on total landscape ET.
- *Climatic variability* – Los Angeles is somewhat unique among cities in that in addition to seasonal variation, there is a large climatic gradient in temperature, humidity, and precipitation within the Los Angeles metropolitan area which will result in different potential and actual ET rates across the region.

- *Irrigation technology* – automated timers have facilitated high rates of irrigation that may be decoupled from current climatic conditions and plant requirements. Newer technologies respond to changing conditions in the soil or the atmosphere with direct measurements of soil moisture or estimates of lawn watering needs from weather based calculations.

Below we review our findings in each of these areas.

4.1.1 Species composition

We utilized constant heat sap flux probes to measure *in situ* transpiration rates of mature urban trees throughout the Los Angeles metropolitan area. This is a relatively straightforward method that has been used extensively in natural forests; however, published transpiration rates of urban trees have been scarce. We report the first measurements of transpiration of urban trees in Los Angeles, most of which are well-irrigated according to our measurements of soil moisture and plant water relations. Figure 2.1 showed the variability in whole tree transpiration across different species experiencing similar environmental conditions in summer. Whole tree transpiration may vary by an order of magnitude depending on the species. Contrary to popular belief, native tree species do not transpire less than non-native species and in fact often have very high transpiration rates, as most tree species native to low elevations of southern California are riparian and are adapted to saturated soil conditions. Our results also challenge common beliefs about Australian species which have been assumed to have very high rates of transpiration, but which were relatively water use efficient in our study. This includes the large and iconic *Eucalyptus grandis*. In general, non-riparian species from climates with high Vapor Pressure Deficit (VPD) appear to be the most water use efficient in Los Angeles. Some of these species, such as *Pinus canariensis*, can withstand very dry soil conditions and require little irrigation. The measured transpiration of an unirrigated, urban stand of *Pinus canariensis* at the Los Angeles Zoo was extremely low, yet this stand provided a large shade canopy.

Species composition had a much smaller effect on the ET of lawns. While we observed some differences in the stomatal conductance of lawn species (shown in Figure 2.11), total lawn ET was fairly insensitive to species composition (Figure 2.12). This is due to differences in mowing heights among lawns that affect leaf area index, and also because lawn canopies of uniform height tend to be fairly uncoupled from atmospheric conditions. In general, ET of lawns was much higher than the total transpiration of the urban forest canopies that we measured.

Finally, it is worth noting that merely replacing mesic with arid-adapted vegetation will not necessarily reduce water consumption unless watering practices and also greatly altered. We found that shrubs originating from desert environments had very high transpiration rates when well watered (Figure 2.2). In fact, species from desert and tropical environments may have similar transpiration and photosynthetic rates when grown under favorable resource conditions. The interaction between species composition and watering practices is a significant factor in water conservation as discussed below.

4.1.2 Spatial configuration of landscape types

We measured the ET of combinations of trees and lawns in addition to pure forest stands and unshaded lawns. We found that the addition of trees to lawn landscapes greatly reduced ET, because shading-related reductions in lawn ET were much larger than the small addition of transpiration constituted by trees (Figure 2.10). The highest ET rates that we measured in Los Angeles were in unshaded lawns; in this land cover ET was close to PET. Somewhat counter-intuitively, adding trees to turfgrass landscapes may be an effective strategy to reduce landscape water consumption; for landscapes where lawns are required for recreation, a combination of trees and turfgrass may be a water saving measure.

4.1.3 Climatic variability

VPD is the driving force for transpiration, and the Los Angeles area experiences a high degree of both spatial and temporal variability in VPD. Simple algorithms and models of ET based on energy balance, such as Penman-Monteith type equations, capture some of this variability. What they do not capture are species-specific stomatal responses to variations in VPD, light, and soil moisture. Some species show strong stomatal closure in response to high VPD, while others show little stomatal regulation, which translates into high transpiration rates at high VPD. Therefore, we provide species-specific model coefficients for the response of transpiration to these environmental factors in Table 2.2. When these stomatal responses are accounted for, transpiration can be fairly well predicted across varying environmental conditions.

4.1.4 Irrigation technology

We tested three lawn irrigation technologies and found that relative to the conventional irrigation timer commonly used in southern California residences, substantial water savings are possible with an irrigation system triggered by a soil moisture sensor (Figure 2.13). In our experiment, this system resulted in a highly efficient water budget in which almost all irrigation water was used for grass ET, rather than lost as runoff or subsurface drainage (drainage is arguably returned to the groundwater supply in recharge, but with a risk of aquifer contamination from fertilizers and pesticides). Irrigation technology is another critical factor in reducing outdoor water consumption, even for landscapes that maintain lawn cover.

4.2 Regional scale models

Urban ET is very difficult to model at large scales. The amount and type of vegetation as well as irrigation practices vary from parcel to parcel, resulting in very "patchy" land cover. Most hydrologic models were developed for natural terrain, and applying these models to cities requires modifications to models. We have shown that urban irrigation increases ET by a factor of 5 or 6 relative to unirrigated grasses in the summer months (Table 3.4 and 3.5). Irrigation as well as the amount of vegetation must be accounted for; one useful method is the application of models that are based on remote sensing data. Satellite products capture the spatial variability in vegetation density through NDVI and in surface energy balance through surface temperature. Various land cover classifications are available that provide additional information about vegetation cover.

The UCLA-ET model used in this study provided reasonable estimates of ET when compared to ground-based measurements (Figure 3.10). The model output and data primarily diverged at very high values of ET measured on the ground; these likely occurred during the very high VPD conditions associated with Santa Ana wind events. During these periods, additional work is necessary on both the measurement method and the model parameters to evaluate the causes of the divergence between the two methods. However, for most conditions, the initial UCLA-ET model and the ground measurements were fairly similar. Combining the observations in this model-data comparison with estimates of the proportion of Los Angeles covered by turfgrass, our calculations suggest that approximately 1/6 of the current water consumption of Los Angeles is allocated to turfgrass ET.

To evaluate scenarios of reductions and additions in urban vegetation on ET, the UCLA-ET model was used with higher and lower values of NDVI (a measure of leaf area) than the current land cover. The model was fairly insensitive to small reductions in vegetation density - a 25 percent decrease in NDVI resulted in only modest reductions in ET in all locations. The effects of larger reductions varied by location - a 50 percent reduction in NDVI resulted in a 34 percent reduction in ET in the hot and dry San Fernando Valley, but only a 13 percent reduction in Santa Monica near the coast. However, absolute ET values were predicted to be much higher in Santa Monica, where household water consumption is quite high, so the absolute water savings would still be substantial. Taking into account all municipal water consumption in Los Angeles, a simple extrapolation suggests a 10 percent reduction in annual city water consumption at a 50 percent reduction in irrigated NDVI.

While this modeling framework is very useful for evaluating large scale scenarios of ET, some aspects of urban outdoor water consumption are not yet possible to incorporate. Critically, the remote sensing products used in this study cannot distinguish among types and species of vegetation, and we have shown that species is very important determinant of urban ET. A next step in fine tuning research on urban outdoor water use scenarios is to make both vegetation types and irrigation practices more explicit. We have received a new grant from the National Science Foundation to continue this work by further integrating ecohydrologic data, water management practices, and a variety of computational modeling methods. However, our current work from the plant to the municipal scale shows the potential for reductions in municipal water use through modifications in outdoor landscaping practices. From species selection to irrigation practices, a variety of effective options are available for landowners to reduce outdoor water consumption.

REFERENCES

- Cayan, D., A. L. Luers, M. Hanemann, G. Franco, and B. Croes. 2006. Scenarios of climate change in California: An overview. California Energy Commission, Public Interest Energy Research Program California Climate Change Center, CEC-500-2005-186-SF.
- Le Comte, D. M., and H. E. Warren. 1981. Modeling the impact of summer temperatures on national electricity consumption. *Journal of Applied Meteorology* 20:1415–1419.
- Gleick, P. H., D. Haasz, C. Henges-Jeck, V. Srinivasan, G. Wolff, K. K. Cushing, and A. Mann. 2003. Waste not, want not: The potential for urban water conservation in California. Pacific Institute for Studies in Development, Environment, and Security.
- Hayhoe, K., D. Cayan, C. B. Field, P. C. Frumhoff, E. P. Maurer, N. L. Miller, S. C. Moser, S. H. Schneider, K. N. Cahill, E. E. Cleland, L. Dale, R. J. Drapek, R. M. Hanemann, L. S. Kalksetin, J. M. Lenihan, C. K. Lunch, R. P. Neilson, S. C. Sheridan, and J. H. Verville. 2004. Emissions pathways, climate change, and impacts on California. *Proc. Natl. Acad. Sci.* 101:12422–12427.
- Kenney, D. S., R. A. Klein, and M. P. Clark. 2004. Use and effectiveness of municipal water restrictions during drought in Colorado. *Journal of the American Water Resources Association* 40:77–87.
- Lehman, R. L., and H. E. Warren. 1978. Residential natural gas consumption: Evidence that conservation efforts to date have failed. *Science* 199:879–882.
- Meyers, T. P. 2001. A comparison of summertime water and CO₂ fluxes over rangeland for well watered and drought conditions. *Agricultural and Forest Meteorology* 106:205–214.
- Ngo, N. S., and D. E. Pataki. 2008. The energy and mass balance of Los Angeles County. *Urban Ecosystems* 11:121–139.
- Pataki, D. E., S. E. Bush, P. Gardner, D. K. Solomon and J. R. Ehleringer. 2005. Ecohydrology in a Colorado River riparian forest: Implications for the decline of *Populus fremontii*. *Ecological Applications* 15:1009–1018.
- Quayle, R. G., and H. F. Diaz. 1980. Heating degree day data applied to residential heating energy consumption. *Journal of Applied Meteorology* 19:241–246.
- Robbins, P., and T. Birkenholtz. 2003. Turfgrass revolution: measuring the expansion of the American lawn. *Land Use Policy* 20:181–194.
- Wilson, K. B., and D. D. Baldocchi. 2000. Seasonal and interannual variability of energy fluxes over a broadleaved temperate deciduous forest in North America. *Agricultural and Forest Meteorology* 100:1–18.
- Wilson, K. B., D. D. Baldocchi, M. Aubinet, P. Berbigier, C. Bernhofer, H. Dolman, E. Falge, C. B. Field, A. Goldstein, A. Granier, A. Grelle, T. Halldor, D. Y. Hollinger, G. Katul, B. E. Law, A. Lindroth, T. Meyers, J. Moncrieff, R. K. Monson, W. Oechel, J. Tenhunen, R. Valentini, S. Verma, T. Vesala, and S. C. Wofsy. 2002. Energy partitioning between latent and sensible heat flux during the warm season at FLUXNET sites. *Water Resources Research* 38:doi:10.1029/ 2001WR000989.

- Allen, R.K., L.S. Pereira, D. Raes, and M. Smith. 1998. Crop Evapotranspiration: Guidelines for computing crop water requirements. Irrigation and Drainage Paper No. 56 FAO, Rome.
- Bijoor, N.S., D.E. Pataki, D. Haver, and J. Famiglietti. 2013. A comparative study of the water budgets of lawns under three management scenarios. In review.
- Goedhart, C. M., and D. E. Pataki. 2012. Do arid species use less water than mesic species in an irrigated common garden? *Urban Ecosystems* 15:215–232.
- Granier, A. 1987. Evaluation of transpiration in a Douglas-fir stand by means of sap flow measurements. *Tree physiology* 3:309–320.
- Litvak E., N.S. Bijoor and D.E. Pataki. 2013. Tree shading reduces plot-scale evapotranspiration from irrigated lawns in a semi-arid urban environment. In review.
- McCarthy, H.R. and D.E. Pataki. 2010. Drivers of variability in water use of native and non-native urban trees in the Greater Los Angeles area. *Urban Ecosystems* 13(4): 393-414.
- McCarthy, H. R., D. E. Pataki, and G. D. Jenerette. 2011. Plant water use efficiency as a metric of urban ecosystem services. *Ecological Applications* 21(8): 3115-3127.
- McLeod, M.K, H. Daniel, R. Faulkner, R. Murison, 2004. Evaluation of an enclosed portable chamber to measure crop and pasture actual evapotranspiration at small scale. *Agricultural Water Management* 67: 15-34.
- Pataki, D. E., H. R. McCarthy, and E. Litvak. 2011. Transpiration of urban forests in the Los Angeles metropolitan area. *Ecological Applications* 21:661–677.
- Phillips, N., A. Nagchaudhuri, R. Oren, and G. Katul. 1997. Time constant for water transport in loblolly pine trees estimated from time series of evaporative demand and stem sapflow. *Trees* 11:412–419.
- Allen, Richard G., A.J. Clemmens, C.M. Burt, K. Solomon, T. O'Halloran, 2005. Prediction Accuracy for Projectwide Evapotranspiration Using Crop Coefficients and Reference Evapotranspiration. *Journal of Irrigation and Drainage Engineering*, Feb, 24-36.
- Bastiaanssen, W.G.M., M. Menenti, R.A. Feddes, and A.A.M. Holtslag. 1998. A remote sensing surface energy balance algorithm for land (SEBAL). Part 1: Formulation. *Journal of Hydrology* 212-213: 198-212.
- Eching, S, and R. L. Snyder, 2005: Estimating Urban Landscape Evapotranspiration, A SCE Proceedings.
- Grimmond, C.S.B., and T.R. Oke, 1999. Evapotranspiration rates in urban areas. Impacts of Urban Growth on Surface Water and Groundwater Quality, IAHS Publication 259: 235-244.
- Johnson, T.D. and K. Belitz. 2012. A remote sensing approach for estimating the location and rate of urban irrigation in semi-arid climates. *Journal of Hydrology* 86-98: 414-415.
- Kim, J and T.S. Hogue. 2008. Evaluation of a MODIS-based Potential Evapotranspiration Product at the Point-scale, *Journal of Hydrometeorology*, 9: 444-460.

- Kim, J., and T.S. Hogue. 2012a. Improving Spatial Soil Moisture Representation through Integration of AMSR-E and Visible and Near-infrared MODIS Products, IEEE Transactions on Geoscience and Remote Sensing 50(2): 446-460.
- Kim, J., and T.S. Hogue. 2012b. Integrating Landsat7 ETM+ and MODIS Products for Improved Spatial and Temporal Surface Flux Estimates. Journal of Applied Remote Sensing 6(1), 063569, doi: 10.1117/ 1.JRS.6.063569
- Litvak E., N.S. Bijoer and D.E. Pataki. 2013. Tree shading reduces plot-scale evapotranspiration from irrigated lawns in a semi-arid urban environment. In review.
- Los Angeles Department of Water and Power. 2011. Urban Water Management Plan. [http:// www.ladwp.com/ ladwp/ cms/ ladwp001354.jsp](http://www.ladwp.com/ladwp/cms/ladwp001354.jsp).
- Mayer, P.W., W. B. DeOreo, E. M. Opitz, J. C. Kiefer, W. Y. Davis, B. Dziegielewski and J. O. Nelson, 1999: Residential End Uses of Water American Water Works Association Research Foundation, Denver, CO. 109p.
- McLeod, M.K, H. Daniel, R. Faulkner, R. Murison, 2004. Evaluation of an enclosed portable chamber to measure crop and pasture actual evapotranspiration at small scale. Agricultural Water Management 67: 15-34.
- McPherson, G., J.R. Simpson, P.J. Peper, S.E. Maco, Q. Xiao, 2005. Municipal Forest Benefits and Costs in Five US Cities." Journal of Forestry 103: 411-416.
- Mini, C., T.S. Hogue, S. Pincetl, J. Kim, D.E. Pataki, T.W. Gillespie, C.G. Boone, J.P. McFadden, G.D. Jenerette. 2013. Single-family residential water use in Los Angeles: Trends and key determinants. In review.
- Rana, G and N. Katerji, 2005. Measurement and estimation of actual evapotranspiration in the field under Mediterranean climate: a review. European Journal of Agronomy 13: 125-153.
- Shuttleworth, W.J. 1993. Evaporation. In: Maidment, D.R. (Ed.), Handbook of Hydrology. New York: McGraw-Hill, pp 4.1-4.53.
- Stannard, D.I., 1988. Use of a hemispherical chamber for measurement of evapotranspiration." Open-File Report, United States Geological Survey, Denver, CO, 88-452.